WSRC-TR-2000-00444

Celotex® Structural Properties Tests

A. C. Smith and P. R. Vormelker
Westinghouse Savannah River Company
Aiken, SC 29808

This document was prepared in conjunction with work accomplished under Contract No. DE-AC09-96SR18500 with the U.S. Department of Energy.

1.0 Background

In the course of regulatory review of the 9975 packaging, the question of the effects environmental conditions on performance of the packaging was raised. The results of previous tests of the Celotex® material, used for impact absorption and thermal insulation, indicated that the effect of temperature variation was small. Accordingly, performance under ambient conditions was judged to be representative of performance under temperature extremes. To extend the data base to include other effects, and in response to the questions, a series of materials tests were performed on the Celotex® brand cellulose fiberboard material.

Keywords: 9975 Shipping Package, Celotex®, Cane Fiberboard

2.0 Test Program

The test program was planned to obtain data on Celotex® performance at extremes of temperature and humidity, Reference 1. Previous experience has shown a rate dependence in impact loading of Celotex® that

has been attributed to the inability of interstitial air to escape during impact loading. As a result, the Celotex® appears more stiff under impact loading conditions. To obtain information on this effect, both impact and slow strain-rate tests were performed. Because package overpacks are assembled by building up the cellulose fiberboard material components from sections cut from sheets, laminated specimens were tested with the load applied perpendicular to the plane of the Celotex® sheets and parallel to the plane of the sheets.

In packaging applications, the overpack material is subjected to crush (compression) loadings. However, to provide general insight into the behavior of cellulose fiberboard material, a series of tensile tests was included in this study. The tensile tests were performed using ASTM "dog bone" specimens cut from sheets of Celotex®. Sets of specimens were cut with orientations 90° apart to test for in-plane variation in properties. Single layer tensile specimens were tested with load direction perpendicular to the plane of the Celotex® sheet. Multiple layer tensile specimens were tested with the load direction perpendicular to the plane of the Celotex® sheets and with the load parallel to the Celotex® sheets.

During testing, it was noted that lateral expansion (bulging) of the specimens did not occur. In the absence of this bulging, laterally constrained tests were not needed. However, following post test evaluation showing that the specimens loaded parallel to the plane of the Celotex® sheets failed by buckling, two laterally constrained tests were performed with load parallel to the plane of the Celotex® sheets.

The tests performed in the initial phase of the test program are summarized in the following tables.

Table 1. Slow Strain Rate Tests

Tensile Tests

Test A. Tensile test parallel to sheet.
Temperature: Ambient & 250°F

Test B. Tensile test perpendicular to sheet.
Temperature: Ambient & 250°F

Test C. Desiccated tensile test parallel to sheet.
Temperature: Ambient & 250°F

Test D. Desiccated tensile test perpendicular to sheet.
Temperature: 250°F

Test E. Moist tensile test parallel to sheet.
Temperature: Ambient & 250 °F

Test F. Moist tensile test perpendicular to sheet.
Temperature: 250°F

Compression Tests

Test G. Compression test parallel to sheet.
Temperature: -40 °F, Ambient, 250°F

Test H. Compression test perpendicular to sheet.
Temperature: -40 °F, Ambient, 250°F

Test I. Desiccated compression test parallel to sheet.
Temperature: -40 °F, 250°F

Test J. Desiccated compression test perpendicular to sheet.
Temperature: -40 °F, 250°F

Test K. Moist compression test parallel to sheet.
Temperature: -40 °F, 250°F

Test L. Moist compression test perpendicular to sheet.
Temperature: -40 °F, 250°F

Additional Tests:

Laterally Constrained Tests
Temperature: 75°F

Preconditioning: Preconditioning according to ASTM D 4332 with limits specified above.

Table 2. Impact Tests

Test 1. Compression test parallel to sheet.				
	Temperature:	-40°F	CT21	CTV
		Ambient	CT07	
		250°F	CT02	CT04
Test 2. Compression test perpendicular to sheet.				
	Temperature:	-40°F	CT30	CT38
		Ambient	CT05	
		250 °F	CT18	CT26
Test 3. Desiccated compression test parallel to sheet.				
	Temperature:	-40°F	CT17	CT13
		Ambient	CT01	CT03
Test 4. Desiccated compression test perpendicular to sheet.				
	Temperature:	-40°F	CT08	CT10
		Ambient	CT24	CT23
Test 5. Moist compression test parallel to sheet.				
	Temperature:	-40°F	CT06	CT16
		Ambient added	CT11	CT15
		212°F	CT31	CT35
Test 6. Moist compression test perpendicular to sheet.				
	Temperature:	-40°F	CT14	(No Data)*
		Ambient added	CT09	CT12
		212°F	CT19	CT29
Additional Testing Not in Original Plan				
Test 3. Desiccated compression test parallel to sheet.				
	Temperature:	250°F	CT20	CT33
Test 4. Desiccated compression test perpendicular to sheet.				
	Temperature:	250°F	CT34	CT36

*DAS trigger did not function.

3.0 Test Apparatus and Data Acquisition

In each case, the specimens conformed to ASTM C-208 and were prepared and tested in accordance with ASTM C-209, References 2 and 3.

The slow strain-rate tests (i.e., those conducted at a normal rate for materials testing) were performed using a Sintech 4507 testing machine fitted with an environmental chamber. Load and displacement data for the slow strain rate tests were recorded using the calibrated load cell and extensiometer installed on the test machine. The strain rate was 2 in. per minute, per the ASTM standard.

The impact tests were performed on a Instron falling beam impact test machine. The impact load is provided by a horizontal beam which is guided by four columns. The weight of the falling beam is 580 lb_f. All tests were performed using a drop height of 60 in., which results in an impact velocity of 17ft/sec. For the environmentally conditioned tests, the specimens were preconditioned in the appropriate environment and then placed in the machine and tested immediately.

The acceleration of the falling beam was measured using an accelerometer. The accelerometer had a sensitivity of 9.95 mv/g with a linear range of 10 Hz to 18 kHz. A 6 pole low pass analog anti-aliasing filter was set for a 2.5 kHz corner frequency. Data was acquired using a 12 bit sampling over a +/- 5 v range.

The data acquisition system (DAS) software records 4096 data points. The maximum duration is 100 ms, so the sample rate becomes 4096 samples in 0.1 sec. Sampling is initiated by an emitter/ detector with a pair of blades 1.5 cm apart. The emitter/detector provides initial velocity and position. The DAS logged acceleration and time.

Data reduction was performed using Microsoft Excel. An Fast Fourier Transform (FFT) was performed on the signal. The highest frequencies, associated with vibrations of the structure, were cut-off and an inverse FFT was performed. This signal conditioning resulted in a smoother data trace. Excel was used to perform the conversion from volts to acceleration. The output is multiplied by mass of the falling beam to determine the force and integrated to obtain the displacement.

4.0 Testing

A review of the prior data on Celotex® properties showed that the properties were typically very consistent from one specimen to another. Accordingly, minimal replicate tests were required. The test plan typically employed two replicates for preconditioned test conditions. Ambient conditions which duplicated existing data, were generally limited to a single specimen.

The slow strain rate test specimens requiring preconditioning for temperature and humidity were preconditioned in an environmental chamber, then transferred to the test machine and tested immediately. The impact tests specimens were preconditioned in separate chambers. For testing they were transferred to the test machine and tested immediately. Dimensions and weights were recorded before and after preconditioning.

Standard tensile specimens were cut from a sheet of Celotex® so that some were at right angles to the others to capture any the in-plane strength variation. The tensile specimens for loading perpendicular to the plane of the Celotex® sheets were bonded to wood blocks, per the ASTM recommended practice. Multi-layer tensile specimens were also bonded to wood blocks for both loading perpendicular and parallel to the plane of the Celotex® sheets.

Compression tests and laminated tensile tests were performed with specimens oriented in two directions. Those designated "horizontal" were placed in the testing machine so that the load was applied perpendicular to the plane of the Celotex® sheets. Those designated "vertical" were placed in the testing machine so that the load was applied parallel to the plane of the sheets.

For the slow strain-rate tests, the specimens were 2 in. cubes. The dry specimens were prepared by holding them in an oven for 24 hrs, at near 0% relative humidity. The moist specimens were held in a near 100% relative humidity environment for 24 hrs.

For the impact tests, the specimens were 4 in. cubes. The larger size, compared to the slow strain-rate tests, was required to insure that the effect of trapped interstitial air on specimen stiffness was captured. Because of the larger size, longer preconditioning exposure was required. The hot desiccated specimens were oven dried to 67 hrs at 250°F, then cooled in a chamber with anhydrous calcium sulfate desiccant for 27 hrs before testing. The cold specimens were oven dried for 26 hrs, then placed with desiccant and cooled for 18 hrs, to ambient temperature, chilled in a freezer for 48 hrs and finally chilled to -40°F using dry ice. The moist specimens were placed in an insulated chamber with containers of boiling-temperature water. The water was periodically replenished, and the specimens were weighed. When the specimens showed no further weight gain they were tested. Humidification process typically took over four days.

5.0 Results

The compression test results are shown in Figures 1 through 40**.** The results of the tensile tests are shown in Table 3 and Figure 41.

5.1 Compression Tests

The compression test data obtained was compared with the reference information on Celotex®, contained in the Oak Ridge report, Reference 4, and date obtained in testing at SRS, Reference 5. The results of the slow strain rates tests conducted at SRS are very consistent with the Oak Ridge and earlier SRS results. The curves have the same form, are nearly coincident, cross one-another at some points and have a maximum difference in values of less than 20% in the steeply rising part of the curves. The high and low temperature tests results were also very consistent with the Oak Ridge results, Figures 1 and 2. The data shows conclusively that the previous data base applies to the Celotex® employed in this study (which was procured for the current production of 9975's). For reference, the comparison between these data and the data referenced in the OakRidge report and the 9975 SARP is shown in Figure 1.

The behavior of the material with respect to orientation (load perpendicular to Celotex® sheets vs load parallel to sheets) was evaluated for impact and normal strain rate conditions, Figures 3 and 4. Under normal (slow) strain-rate test conditions, the perpendicular loading orientation is typically 3 to 4 times as stiff as the parallel loading orientation, in the region above 50% strain, Figure 3. Likewise, for impact loading, the perpendicular loading orientation is 3 to 4 times stiffer than the parallel loading orientation, in the region above 50% strain, Figure 4. In all cases, the specimens tested with load perpendicular to the sheets crushed uniformly without lateral bulging. In all cases, the specimens tested with load parallel to the sheets, and without lateral restraint, buckled early in the loading process, then crushed when additional buckling deformation could not occur. Perpendicularly loaded specimens crush progressively with rapid increase in the slope of the stress strain curve as the porosity (void) is closed in the specimen. (This condition is called "lock-up" in the literature.) Onset of lock-up is delayed for parallel loaded specimens by the buckling process, which results in lower values of stress values for given strains. Upon onset of lock-up, the stress-strain curve turns rapidly upward, like that for the perpendicular load case.

Slow strain rate tests were performed, on 2 in. cube specimens with load parallel to the plane of the Celotex® sheets, using the lateral constraint fixture to determine behavior when bulk buckling is prevented. These results showed that, following the initial buckling of the glue layers, the Celotex® crushing stress-strain behavior is very similar to the results for unconstrained specimens loaded perpendicular to the sheets, Figure 5.

The effect of strain rate was found to be significant. Impact stresses were typically 3 times those for the corresponding normal (slow) strain-rate results, in the region above 50% strain, for perpendicular loading, Figure 6. For the parallel load orientation, the impact stresses were typically 4.5 to 6 times those for slow strain-rate tests, in the region above 50% strain, Figures 7.

The tests conducted at high (250°F) and low (-40°F) temperatures were generally consistent with earlier Oak Ridge results, Figure 8. For the normal (slow) strain-rate tests, the hot and ambient results were very close. The cold specimens proved somewhat stiffer (by a factor of about 1.5, for the perpendicular load orientation) than the ambient specimens, in the region above 50% strain, Figures 9 and 10. The difference for the parallel orientation was greater (the difference being a factor of around 2), for the region above 50% strain. The earlier Oak Ridge low temperature results did not show this difference, Figures 8 and 11. The high temperature impact stresses, for loading perpendicular to the plane of the Celotex®, were around 3 times as great as the corresponding high temperature slow strain-rate results, for the region above 50% strain, Figure 12. In the corresponding case for loading parallel to the plane of the Celotex®, the impact stresses were 3 to 5 times greater, Figure 13.

The cold (-40) slow strain-rate comparison for load perpendicular and parallel to the sheets, shown in Figure 14,

is similar in character to the ambient results (Figure 3). However, the difference between the perpendicular and parallel results is not as great for the low temperature case.

The environmental conditioning included drying some of the specimens and extended exposure of others in a water saturated chamber (near 100% relative humidity). For the normal strain-rate case, the dry specimens behavior was little different from the ambient condition, reference specimens. The humidified specimens typically were somewhat less stiff than the dry or ambient specimens (by a factor of 0.8, typically), for the region above 50% strain, for the perpendicular loading orientation, Figures 15 and 16. For the vertical orientation (load parallel to plane of Celotex® sheets), there is no significant difference between moist and ambient results at low temperature (-40F), Figure 17. For loading perpendicular to the sheets, the high temperature moist case proved less stiff than the ambient and low temperature specimens, Figure 18. Comparison of the parallel and perpendicular load results for the cold, moist cases, showed the perpendicular load case was typically stiffer than the parallel load case by a factor of 2 for strain above 50%, Figure 19.

The dry impact test results show the perpendicular load case is typically around 6 times as stiff as the parallel load case, for the region between 50% and 70% strain. For the parallel loading cases, stress increases rapidly for large strain (above ~0.5), Figure 20. The parallel load cases typically have a small, transient peak, early in the deformation process. One of the dry, parallel impact specimens (CT01) displayed a significant peak at the start of the deformation.

The slow strain-rate results (both Oak Ridge and SRS) also show a small peak early in the deformation process for the parallel load cases, e.g., Figure 2. These specimens (loaded parallel to the plane of the Celotex® sheet) failed by buckling, with the peak being attained just before buckling began. None of the slow strain-rate cases with load perpendicular to the Celotex® sheets displays a similar response. The initial peak effect resulted in early termination of some slow strain-rate tests, when the stress fell below half of the peak stress, triggering the automatic shutoff for the test machine. The mechanism causing the peaks is discussed below.

For the impact tests, the stiffness of the moist specimens was less than one-half that of the dry or ambient specimens. This difference, compared to the slow strain rate cases, may be attributable in part to differences in method of exposure to the humid environment.

Cold dry samples are typically stiffer than cold moist samples (by a factor of about 1.2), Figure 16. Comparison of Figures 17 and 18 show that the cold moist samples are typically more stiff than the ambient or hot moist samples. In the cold, moist condition, the specimens are stiffer for perpendiculal loading than for parallel loading, Figure 19.

Comparison of impact tests for loading perpendicular to the plane of the sheets indicated that the ambient conditions specimen was stiffer that the cold specimen, Figure 21. The impact tests of some cold specimens, for parallel load cases, showed an initial high, very short duration peak stress, Figure 22. The similar spike, seen on one of the dried specimens (Figure 20), was noted above. The duration of the spike is on the order of a few milliseconds, in all cases. This effect is discussed below.

The comparison of the low temperature, parallel load impact test results, for dry and ambient cases is shown in Figure 19. All of the curves show a similar form, with the early peak followed by low stress until the strain approached 50%. After this point the stress rises abruptly. The curve for test CT17 displays a much lower initial peak, with the onset in the rise in stress taking place when the strain approaches 70%.

The initial peak is not found for the corresponding, low temperature, perpendicular load. For example, CT30 shows no initial peak, and the stress rises more progressively for strains greater than 40%, Figure 23. As these

results indicate, the initial peak is not experienced in every low temperature case.

Comparison with results for test CT21, Figure 22, illustrates the difference in response for specimens having an initial peak. Because of the energy absorbed in crushing in the initial peak, specimens with an initial peak display an earlier and more rapid rise in stress as strain increases beyond 50%. This is illustrated in Figure 22, where the specimen with the higher peak displays an early and steeper rise in stress for strain above 50%. The preconditioning for the two specimens shown in Figure 22 was identical.

Figures 23 and 24 compare the results of low temperature impact and slow strain-rate results for the perpendicular loading case for ambient-moisture and dried specimens. For these low temperature cases, there is little difference in the impact and slow strain-rate results.

The variation in magnitude of the initial peak, for specimens with the same preconditioning, is illustrated in Figure 25.

The comparison of parallel load case impact test results for dry, ambient and moist specimens is shown in Figure 26. The initial peak for the dry specimen (CT01) is associated with earlier rapid rise in stress (lock-up) than for the ambient and moist specimens. The moist specimen (CT11) crushes uniformly, but is less stiff than the ambient or dry specimens. The corresponding comparison for the perpendicular load case is shown in Figure 27. In the absence of an initial peak, the dry and ambient moisture cases are quite close. The moist specimen is significantly less stiff than the dry and ambient cases.

Comparison of the cold, moist impact results for loading parallel to the sheets is shown in Figures 28 and 29. Although the cold, moist specimens display a small initial peak, the effect is much less pronounced than for the dry case.

There is about a 10% variation, from specimen to specimen, for the slow strain rate tests. The difference for the impact tests is greater.

5.1.1 Second Series Impact Tests

In the course of the impact testing, mechanical problems were experienced with the test machine, caused by vibrations attributed to an insufficiently rigid foundation. The machine was repaired and relocated onto a new foundation, consisting of a 5 ft cube of reinforced concrete. The original test matrix was completed and several additional tests, requested by the review team, were performed. The results of this second series of tests are shown in Figures 30 through 40. Only the anti-aliasing filter was used for these results.

The preconditioning for Figure 30 is the same as for specimen CT21 in Figure 22. The preconditioning for Figure 31 (CT38) is the same as for CT30 in Figure 24. Figures 32 and 33 provide results for impact tests of hot, moist specimens loaded parallel to the plane of the Celotex sheets. Figure 34 shows results for CT14, a -40° F, moist specimen loaded perpendicular to the plane of the Celotex. The corresponding hot, moist cases for perpendicular loading are shown in Figures 35 and 36. Figures 37 and 38 (for CT20 and CT33) show results for hot, desiccated specimens loaded parallel to the plane of the Celotex sheets. These may be compared with the results for CT01, Figure 20. The complementary hot, desiccated tests with load perpendicular to the plane of the Celotex sheets are shown in Figures 39 and 40 (Specimens CT34 and CT36).

The results of these tests are, for the most part, qualitatively similar to those from the first series of impact tests. The tests for the cases where glue stiffening would be expected (hot, desiccated or -40°F), and the load is parallel to the sheets, the high initial stress displayed in the earlier results is found. In these tests, however, the initial spike is followed by a series of progressively lower spikes. At the onset of "lock-up", the stress strain

curve turns rapidly upward, as in the previous results (Figures 30, 37 and 38). These cases are characterized by fragmenting of the specimens.

The response for cold, ambient moisture specimen CT38 (Figure 31) is similar in character to its counterpart from the first series of tests, CT30, Figure 24. However, while the peak stress remains unchanged, the deformation at which lock-up is experienced is on the order of 12% where in the earlier testing it occurred at about 40%. The peak stress in Figure 31 is at about 30% strain. The corresponding cold, moist case (CT14), for perpendicular loading is shown in Figure 34. The peak stress is comparable, but on-set of lock-up occurs at about 20% strain and the peak stress occurs at about 40% strain.

Under hot, moist conditions, the glue stiffening effect would not be expected to occur. The specimens with hot,moist preconditioning loaded parallel to the Celotex® sheets, Figures 32 and 33, are found, as expected, to behave similarly to specimens loaded perpendicular to the Celotex® sheets. The results are similar in character to earlier data for moist specimens (e.g., CT11, Figure 26) except, like the new results for perpendicular loading, lock-up is shown at about 20% strain rather than >50% shown in Figure 26.

The comparable hot,moist specimens loaded perpendicular to the Celotex® sheets (Figures 35 and 36) are, likewise, very similar to the earlier results, CT09 in Figure 27, with the peak stress occurring at lower strain (45% compared to 75% for CT09) than the earlier results.

Finally, the results for the hot, desiccated specimens loaded perpendicular to the Celotex® sheets (Figures 39 and 40) are similar to those for the earlier ambient temperature, desiccated test, CT24, Figure 27. As with the other tests in the second series, the peak stress occurs earlier, around 35% strain compared to 75% for CT24.

5.2 Tensile Tests

The tensile tests of "dog bone" specimens showed scatter on the order of 20% in the results. This scatter is attributable in part to the specimen geometry. Several specimens did not fail in the reduced section.

The comparison of tensile specimens cut at right angles (labeled "longitudinal" and "transverse") showed somewhat higher tensile strength for the longitudinal specimen under ambient conditions and for the higher transverse specimen under dry-room temperature conditions. The scatter in values for other cases suggested that this difference was not significant. The tensile strengths for the longitudinal and transverse cases for 250°F-ambient humidity were quite close. The tensile strengths for the 250°F-dry, moist-room temperature, and 250° F-moist cases also had similar values. A typical load-deflection curve for these Celotex® tensile tests is shown in Figure 41.

Review of the data suggests that the direction, longitudinal vs transverse, had no significant effect on the tensile strength of the Celotex®. The tensile strength was not strongly affected by increase in temperature, for the duration of the test. Likewise, dry specimens, tested at room temperature showed no loss in tensile strength. A typical value for these cases was around 170 psi.

The dry specimens, tested at 250°F were consistently somewhat lower. A typical value for this case was around 140 psi.

The tensile strength for the humidified (moist) specimens was significantly lower for both the ambient temperature and 250°F cases. A typical value for the moist cases was around 90 psi.

The tensile tests for loading perpendicular to the plane of the Celotex® sheets consistently yielded much lower tensile strengths. This was true regardless of preconditioning. Single layer and multi-layer specimens were tested at room temperature-ambient humidity, 250°F-ambient humidity and 250°F-dry. A typical value for the single layer tests, for all of these cases was 13 psi. The multi-layer results were even lower, 4 psi being typical. Two humidified multi-layer specimens were tested at 250°F and found to have a tensile strength of around 2 psi. The multi-layer specimens typically failed at the glue joints.

One multi-layer specimen was tested with load parallel to the plane of the Celotex® sheets. The tensile strength for this specimen was similar to that of the "dog bone" tensile specimens, 158 psi. Other specimens tested in this orientation experienced failure at the glue joint attaching the specimen to the wood block and failure of the wood block itself.

5.3 Density Results

The density results from the Celotex® specimens are given in Table 4.

The density of the material when it leaves the manufacturer is in the range of 14 to 16 lb/ft3 (verified by certified material test report). Specimens in the current test program which have not been glued together, and which have been in stock for about a year, have an average density of 16.8 lb/ft3. For those assembled by gluing layers together, the density values are: 17.9 lb/ft3 (with a lot of variation) for 2 in cubes used for the slow strain tests; and 19.1 lb/ft3 (avg) for the 4 in cubes used for the impact tests.

Moistening the specimens, for the 4 in cubes, increased their density to 19.8 lb/ft3. Drying the specimens reduced their density to 18.5 lb/ft3.

The average decrease in linear dimension ($\Delta l/l$) for each of the desiccated specimens was on the order of 1.5% (i.e., 0.015). The average increase in linear dimension ($\Delta l/l$) for each of the moistened specimens was on the order of 0.3% (0.003).

6.0 Discussion

Past reference to the increase in stiffness of Celotex® under impact strain rate conditions has attributed the effect to the compression of air, retained in the porous matrix. According to this postulate, under slow strain rate conditions, interstitial air would be able to escape and so would not add to the force resisting the compression. An evaluation of the contribution of the interstitial air to the interfacial stress between the impact plate and the Celotex® specimen indicates that this is not the case. For 70% strain, the maximum stress (assuming isentropic compression) contribution for the compressed air retained in the Celotex® is less than 10 psi. This effect is negligibly small for a total stress of between 200 and 5000 psi. Accordingly, pneumatic effects cannot account for the increase in stiffness of the specimens observed in the impact tests.

The tensile results indicate that there is no in-plane directional variation in properties. Similarly, the laterally constrained compression tests show that, once the glue planes buckle, there is little difference in crush behavior of the Celotex® for loading parallel and perpendicular to the plane of the sheets. These results indicate that the Celotex® material is essentially isotropic, with the directional behavior for laminated specimens being the result of the glue reinforcing the cellulose fiber in the glue-permeated zone.

The results of the testing show that Celotex® behaves in a consistent manner over a wide range of temperature

and moisture conditions. The increased apparent stiffness for the impact test cases was within the expected range for this effect. The most significant deviations from this behavior are the low temperature cases and dessicated cases where an initial peak occurs. This phenomenon is discussed in Section 6.1, below.

The high moisture cases required a long exposure to a saturated environment. These conditions would not be experienced by a package in normal handling. Regardless of the likelihood of a package becoming damp, the difference in stiffness of the Celotex® in the moist condition, compared to ambient conditions, is not great. Even in a damp condition, the Celotex® would meet the functional requirements for absorbing an impact. The lower stiffness in the moist condition would result in somewhat lower peak acceleration being imparted to the containment vessels. The lower strength of the moist material was also clearly shown in the tensile tests.

Post test examination of dropped packages typically shows that the Celotex® has experienced local crushing in the immediate vicinity of the contact point, with most of the cross section undamaged. Consequently, the strain experienced in these tests corresponds to values in the lower range of the stress-strain curves (<0.5).

The nature of the crushing process in all cases tested is a relatively low-stress crushing of the material, followed by a rapidly increasing stiffness as the void is closed (this condition is referred to as "lock-up" in literature on crushing of cellular materials). Accordingly, regardless of the condition of the material with respect to temperature or humidity (and the associated variations in stiffness), at a strain of around 50%, the stiffness rises steeply. The results of the post test examinations of dropped packages indicated that the 50% strain point is not attained. If high strains were attained, the increase in stiffness is sufficient that there would appear to be little difference in the "in-service" performance of the material over the range of properties measured in these present tests.

The second series impact tests all are similar in character to the earlier tests, although the change in machine installation has affected the results. The on-set of lock-up consistently occurs earlier in these tests than in corresponding tests from the first series. The peak loads are similar, so that the earlier onset of lock-up would not affect the peak load imparted to containment vessels. The series of peaks found in the parallel loading tests, for the stiff glue cases, are the top parts of a full oscillation (Figure 42). The frequency of the dominant oscillation (5 cycles in 0.011 sec, or 454 hz) is the same as that found for the other stiff, parallel load cases in the second series of tests. Higher frequencies are superimposed on the signal. The oscillations observed during the buckling phase of crushing in some earlier tests (e.g., CT15 and CT17) appear to have the same frequency. Evaluation of the natural frequency of the impact face plate, to which the accelerometer is mounted, indicates that it is the likely source of the oscillation. The accelerometer is attached to the end of the face plate, which is secured near its mid point to the falling beam. Accordingly, the oscillations are not experienced by the Celotex® specimens. In any event, the successive peaks are lower than the initial peak.

The results of the second series of impact tests support the understanding that the cause of the difference in response for loading parallel and perpendicular to the plane of the Celotex® sheets and for the initial spike seen in some cases of loading parallel to the sheets is structural in nature.

The test results show that the tensile strength perpendicular to the plane of the Celotex® is significantly lower than its in-plane strength. In this regard, the material is not isotropic. This is usually not an issue for packaging applications, because drop and handling loadings generally impose compressive loads. For low angle drops, a bending stress is induced in the Celotex® assembly. The low tensile strength perpendicular to the plane of the Celotex® sheets makes formation of radial separations likely under such conditions.

6.1 Mechanism of Initial Spike in Test Results

6.1.1 Test Results

As described above, examination of the slow strain rate results for loading parallel to the sheet shows that, in every case, the stress rises sharply, initially, before reaching a peak on the order of 200 psi, then drops off for an extended period of buckling and crushing. Then, as the void is closed (i.e., at lock-up), the stress strain curve turns rapidly upward. The initial steep rise appears to be an elastic behavior (i.e., linear). In contrast, for loading perpendicular to the plane of the Celotex®, the specimens crushed uniformly, with slowly increasing stress until the void was closed (lock-up). The stress strain curve then turned rapidly upward.

Examination of the impact testing results revealed a high, short duration stress peak (or spike) in the initial phase of crushing of several of the Celotex® specimens (e.g., Figure 22), when the loading was parallel to the plane of the Celotex® sheets. The conditions under which this behavior occurred were a very low temperature (-40°F) and, in one case (CT01), for a desiccated specimen. This behavior was not observed for loading perpendicular to the sheets

6.1.2 Review of Literature

Literature on the behavior of cellular materials under dynamic crushing provide insight into the mechanism leading to the spike in the present results, References 6 through 9.

Open cell behavior is dominated by the structural response of the cell walls. Crushing in such materials depends upon the geometry of the individual elements and inertia. The crushing takes place by local instabilities in deformation of the cell walls. The inertia of the cell walls can modify the local quasi-static mechanism within the structure, leading to less compliant modes of failure and requiring higher loads to cause crushing. Initial peaks are common for (anisotropic) cellular materials with load applied parallel to cell walls. Examples of this are metal honeycombs and woods.

In particular, results for crushing of honeycomb structures, both in the literature and in SRS tests, show high initial peaks, followed by a uniform crushing plateau region termed "progressive buckling". Once buckling extends throughout the structure (lock-up), the stress rises very rapidly.

In addition, in honeycomb crush tests, rounded impactors did not produce the initiating peaks observed in crush tests with flat impactors. This is relavant because in horizontal impact the rounded Celotex strikes a flat surface.

One of the most important features of dynamic crushing of various woods is the enhancement of crush stress. The initial peak, impact loads, plateau loads, and maximum stiffening loads (i.e., those when the material is almost fully crushed) all increase to some degree with the increase in impact velocity.

For dynamic loading of wood, once buckling occurs, there is a dramatic drop from the initial peak down to stress levels that are only slightly increased above the plateau stress for the slow strain-rate case. This is a similar characteristic to that detected in aluminum honeycomb and hexagonal-closest-packed ring systems. This is believed to be caused by local inertial effects (called micro inertia in the literature), which cause buckling to occur at higher modes than for the slow strain rate case.

6.1.3 Summary of behavior

The initial response to loading of cellular structures is elastic, with the stress being carried (elastically) by the cell walls. As the load increases above the point where the walls become structurally unstable, they begin to buckle, with consequent reduction in load carrying ability. As the deformation continues, the buckling

propagates through the material, at a fairly consistent stress level. When essentially all of the cell volume has buckled, the stress increases rapidly. This point is referred to as lock-up.

Under dynamic conditions, the loads in all of these regimes increase as a function of strain rate.

6.1.4 Behavior of bonded Celotex® Specimens

The results of the Celotex® impact tests are fully consistent with the expected behavior, based on examples in the literature.

For loading perpendicular to the plane of the Celotex®, the Celotex® displays no elastic behavior above a few ten's of psi and crushes consistently, with stress rising as lock-up is approached. The glue layers carry no load in this orientation.

The behavior of specimens loaded parallel to the planes of the Celotex® is determined by the glue reinforced layers, which divide the material into 2-D cells. The initial crushing is determined by the glue layers which act as columns, stabilized by the weaker Celotex® interstitial material. The buckling of these glue-reinforced-cellulose-fiber layers causes the entire specimen to buckle, if unconstrained. The buckling dominates the crushing behavior until further buckling cannot occur. Beyond this point, the Celotex® crushes in a manner like that for perpendicular loading, rapidly attaining lock-up.

To further investigate this mechanism, an ABAQUS model of the impact test specimens was developed and a parametric study performed, Reference 10. The results confirm that the glue layers are responsible for the difference in crush performance of the impact test specimens between loading parallel and perpendicular to the Celotex® sheets. The results of this study were used to develop a finite element model of the package to evaluate the effect of the glue stiffening on the acceleration experienced by the containment vessels during a regulatory 30 ft drop.

6.1.5 Effect of Environmental Conditioning

The spike is observed in low temperature cases and in one desiccated case. The glue in question is Elmers' Carpenter's Glue, which is a modified polyvinyl acetate emulsion very similar to water based white glue used for joining paper, etc. It is a matter of experience that this glue bond is strongest when it is well dried. This would account for the occurrence of the modest spike for the desiccated case (CT01). In addition, the manufacturer reports that this glue becomes stiff, or brittle at sub-freezing temperatures. This would account for the occurrence of the spike in the low temperature tests. Under conditions where the glue is more flexible (higher temperature and humidity) the effect would be minimal.

6.1.6 Factors Affecting Magnitude and Duration of Initial Peak

The factors affecting the magnitude and duration of the initial spike are those which affect the rate of strain and the buckling behavior of the glue layers.

The rate of strain is determined by impact velocity.

Buckling is determined by the structural characteristics of the glue-layer cells (filled with Celotex®). The important characteristics are the thickness and spacing of the glue layers and the structural properties of the glue layers. The structural properties of the glue layers depend upon whether the glue is acting as a relatively soft

visco-elastic material (moderate temperatures and humidity) or as a relatively stiff elastic material (very dry or cold conditions).

6.1.7 Consequences for the 9975 Packaging Application

Because the loading for axial drops is perpendicular to the plane of the Celotex® sheets, this phenomenon would have no effect on the results of axial drops, which are the most severe in transmitting accelerations to the containment vessels. For the various corner drops, which are low acceleration drops in any event, the loading on the glue layers is out of plane, so the effect of the stiffening would be minimal.

Only horizontal impacts, where the loading is parallel to the plane of the Celotex® would be affected by the stiffening effect of the glue joints. However, the horizontal impact is radial to the circular cross-section of the package. Since the crush affected area increases progressively, the horizontal impact produces less severe accelerations than the axial cases.

The finite element analysis of the 9975 during a 30 ft horizontal drop revealed that the glue stiffening effect is bounded by the acceleration caused by the crushing of Celotex®, Reference 11. The analysis used the results of the impact test ABAQUS model mentioned above. The presence of stiff glue layers results in a peak early in the impact event. However, the maximum acceleration occurs later in the process when crushing has progressed so that a large region of Celotex® is involved. The maximum acceleration was found to be comparable to that for the case where glue stiffening is not present (i.e., ambient conditions). The peak acceleration is less than that assumed for the structural analysis of the containment vessels.

7.0 Conclusions

The results of the tests reported here are consistent with the data used for the design calculations for the 9975 package.

These test results indicate that the performance of the Celotex® under ambient conditions is representative of its performance under most environmental conditions, for deformations experienced in package applications.

The occurrence of the spike is the result of the stiffening of the glue layers at low temperature.

The nature of the compression stress-strain curves indicates that the material will fulfill its functional requirements, even under the most adverse environmental conditions.

8.0 References

1. Smith, A. C., "9975 Drop Test Task Plan", SRS Letter SRT-RMPT-2000-00010, Feb. 29, 2000.
2. ASTM Standard C-208, Standard Specification for Cellulosic Fiber Insulating Board.
3. ASTM Standard C-209, Test Methods for Cellulosic Fiber Insulating Board.
4. Walker, M. S., *Packaging Materials Properties Data*, Oak Ridge report Y/EN-4120, Jan. 1991
5. *Safety Analysis Report – Packages, 9965, 9968, 9972-9975 Packages*, Westinghouse Savannah River Co. Report WSRC-SA-7, Rev. 10, 2000.
6. Jones, N. and Wierzbicki, T., Eds, Structural Crashworthiness and Failure, Chap. 8, Dynamic Compression of Cellular Structures and Materials, Elsevier Applied Science, London, 1993.
7. Easterling, K. E., Harryson, R. Gibson, L. J., and Ashby, M. F., On the Mechanics of Balsa and Other Woods, Proc. R. Soc, London, A383, pp 31-41, 1982.

8. Leader, D., Honeycomb Crush Test Results, SRS memorandum, Leader to Cadelli, June 28, 1995.
9. Product Data Sheet: Elmer's Professional Carpenter's Wood Glue, Elmer's Products,Inc. Columbus,OH.
10. Gong, C., *Computational Parametric Analysis of Mechanical Behaviors of Celotex Implanted with Glue Plates*, Westinghouse Savannah River Co. Calculation Note M-CLC-F-00689, December 4, 2000.
11. McKeel, C., *Celotex Glue Stiffening Effects on 9975 Shipping Container Drop Performance (U)*, Westinghouse Savannah River Co. Calculation Note T-CLC-F-00195, December 14, 2000

Acknowledgments

The authors wish to recognize G. Chapman and G. Creech, who performed the testing at SRS, and K. Miller of the University of South Carolina, for their conscientious support. Mr. Miller performed the impact testing at USC, under the direction of Dr Jamil Khan and Dr. Curtis Rhodes of the Mechanical Engineering Department of the University of South Carolina.

Table 3. Tensile Properties of Celotex

Test Type	Pre-Conditioning at % Relative Humidity	Sample ID	Orientation	Actual Test Temp. C	Peak Load (lbs.)	Ultimate Stress (psi)	Elongation at Break %	Failure location
Dogbone Tensile	Ambient/no pre-cond.	1L	Longitudinal	24.1 RH45	137.52	190.24	0.0609	reduced sect.
Dogbone Tensile	Ambient/no pre-cond.	2L	Longitudinal	120.90	113.37	156.63	0.0627	reduced sect.
Dogbone Tensile	Ambient/no pre-cond.	3L	Longitudinal	120.10	122.15	170.30	0.0682	reduced sect.
Dogbone Tensile	0% RH	9L	Longitudinal	24.10	124.77	172.82	0.04	reduced sect.
Dogbone Tensile	0% RH	6L	Longitudinal	122.00	97.38	140.19	0.0514	radius
Dogbone Tensile	0% RH	10L	Longitudinal	122.40	101.76	138.16	0.0460	radius
Dogbone Tensile	0% RH	12L	Longitudinal	121.00	110.14	154.61	0.05	reduced sect.
Dogbone Tensile	100% RH	7L	Longitudinal	25.00	65.06	90.04	0.0966	reduced sect.
Dogbone Tensile	100% RH	8L	Longitudinal	125.20	75.73	103.45	0.1102	grip
Dogbone Tensile	100% RH	11L	Longitudinal	121.90	52.25	72.37	0.1479	grip

Dogbone Tensile	Ambient/no pre-cond.	1T	Transverse	24.10	108.71	151.15	0.0684	reduced sect.
Dogbone Tensile	Ambient/no pre-cond.	2T	Transverse	122.10	103.60	147.00	0.0561	reduced sect.
Dogbone Tensile	Ambient/no pre-cond.	3T	Transverse	120.60	109.04	153.82	0.0510	reduced sect.
Dogbone Tensile	0% RH	6T	Transverse	122.90	104.83	150.91	0.0457	reduced sect.
Dogbone Tensile	0% RH	11T	Transverse	121.00	86.83	120.73	0.0512	reduced sect.
Dogbone Tensile	0% RH	12T	Transverse	121.00	96.55	135.53	0.0814	reduced sect.
Dogbone Tensile	0% RH	7T	Transverse	25.10	36.21	50.83	0.0995	reduced sect.
Dogbone Tensile	0% RH	9T	Transverse	24.10	131.47	188.53	0.0444	reduced sect.
Dogbone Tensile	100% RH	8T	Transverse	120.40	77.18	109.20	0.0682	reduced sect.
Dogbone Tensile	100% RH	10T	Transverse	120.90	61.06	86.03	0.0817	reduced sect.
S-layer Tensile	Ambient/no pre-cond.	1	Perpendicular	24.20	68.97	16.3	0.0297	in fiber
S-layer Tensile	Ambient/no pre-cond.	2	Perpendicular	122.40	37.21	8.85	0.0275	in fiber
S-layer Tensile	Ambient/no pre-cond.	3	Perpendicular	122.40	43.05	10.24	0.0337	in fiber
S-layer Tensile	0% RH	4	Perpendicular	121.70	55.42	13.19	0.0231	in fiber
S-layer Tensile	0% RH	5	Perpendicular	121.20	52.88	12.71	0.0238	in fiber
M-layer Tensile	None	1	Perpendicular	ambient	21.51	4.97	0.0598	glue joint
M-layer Tensile	None	2	Perpendicular	122.90	14.28	3.35	0.0865	in fiber

M-layer Tensile	None	3	Perpendicular	121.50	5.07	1.19	0.0682	glue joint
M-layer Tensile	0% RH	4	Perpendicular	121.40	22.08	5.25	0.0276	glue joint
M-layer Tensile	0% RH	5	Perpendicular	121.50	16.54	3.88	0.024	glue joint
M-layer Tensile	100% RH	6	Perpendicular	122.20	3.26	0.76	0.0567	glue joint
M-layer Tensile	100% RH	7	Perpendicular	121.80	11.72	2.75	0.0486	joint & fiber
M-layer Tensile	None	1	Parallel	amb	685.04	157.58	0.049	in fiber& glue jt.

Table 4. Density of Test Specimens

As manufactured (per CMTR)		14 – 16 lbm/ft^3
Slow Strain Rate Specimens		
	Single Layer specimens*	16.8 lbm/ft^3
	Multi Layer specimens	17.9 lbm/ft^3
USC Impact Test Specimens		
Density		
	Ambient moisture	19.1 lbm/ft^3
	Humidified	19.8 lbm/ft^3
	Desiccated	18.5 lbm/ft^3
Dimensional Change		
	Humidified	0.3%
	Desiccated	1.5%

* Fabricated from material in stock for about a year.

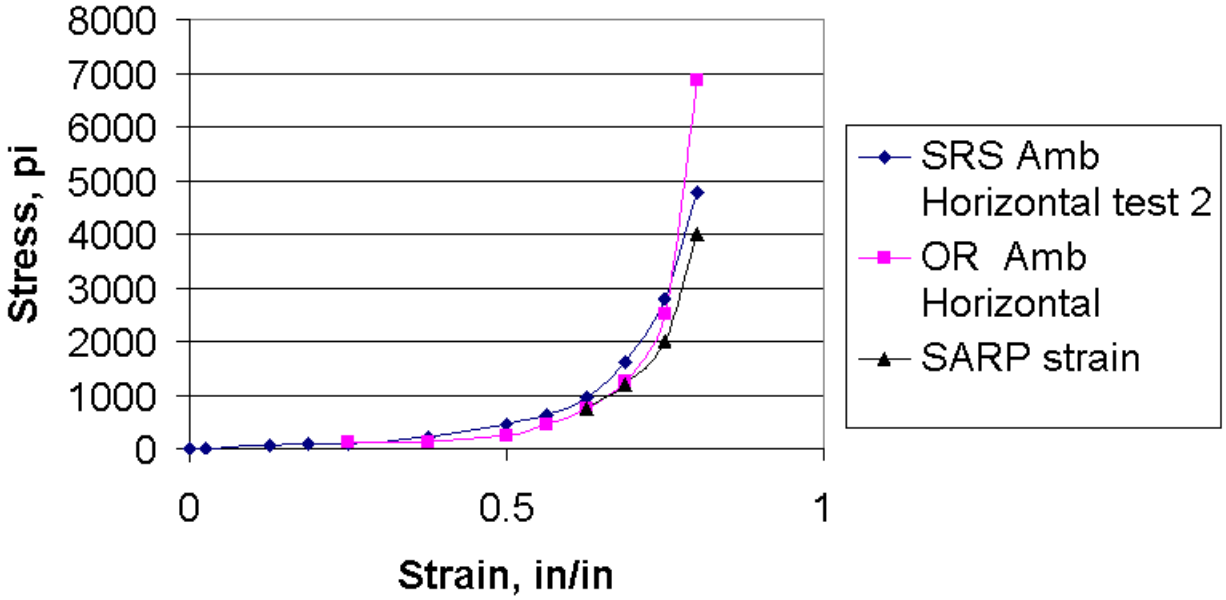

Figure 1. Comparison of SRS Results With Oak Ridge and SARP Data.

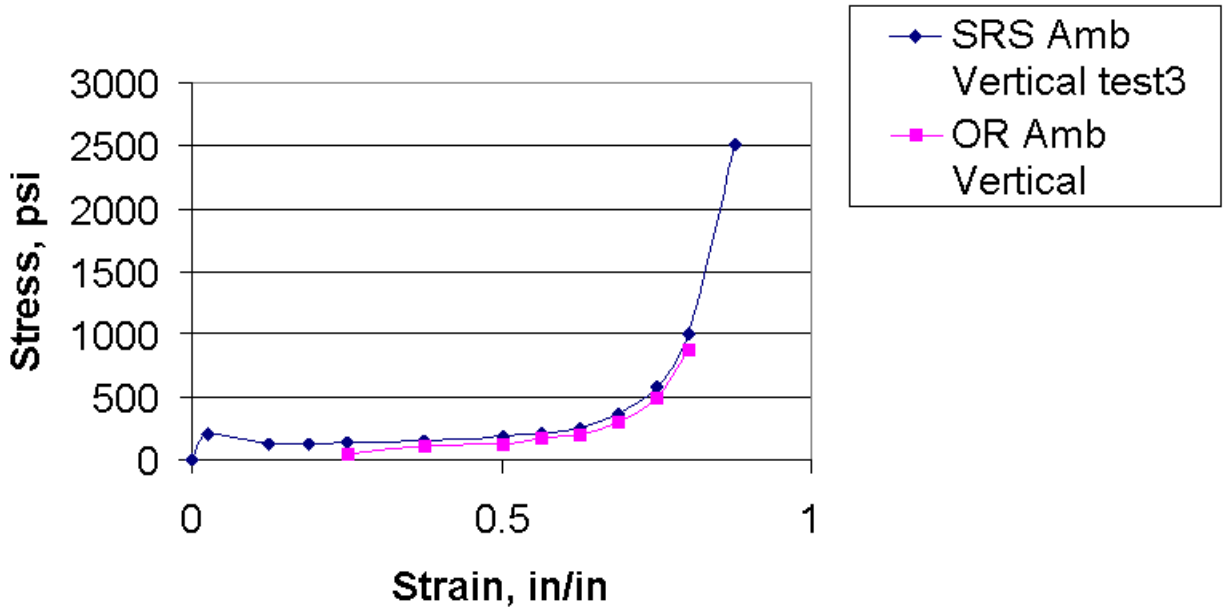

Figure 2. Comparison with Oak Ridge Data for Load Parallel to Plane of Celotex Sheets

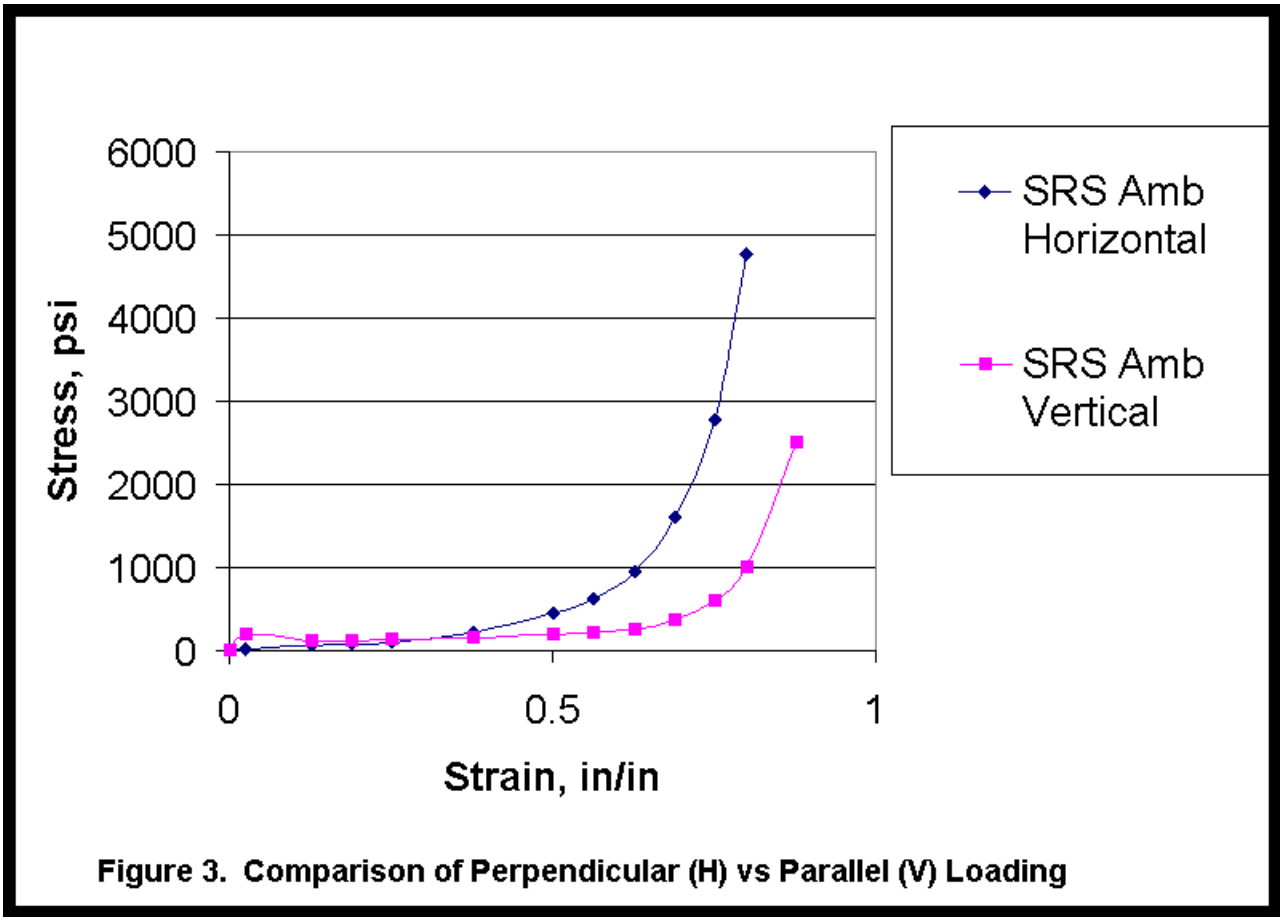

Figure 3. Comparison of Perpendicular (H) vs Parallel (V) Loading

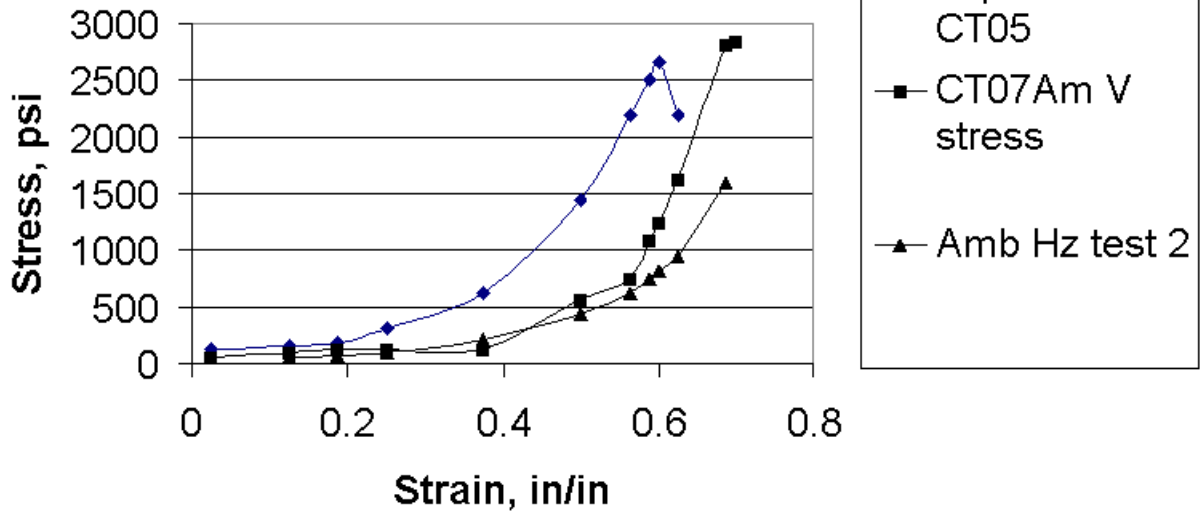

Figure 4. Comparison of Results of Impact Perpendicular and Parallel to the Plane of the Celotex Sheets.

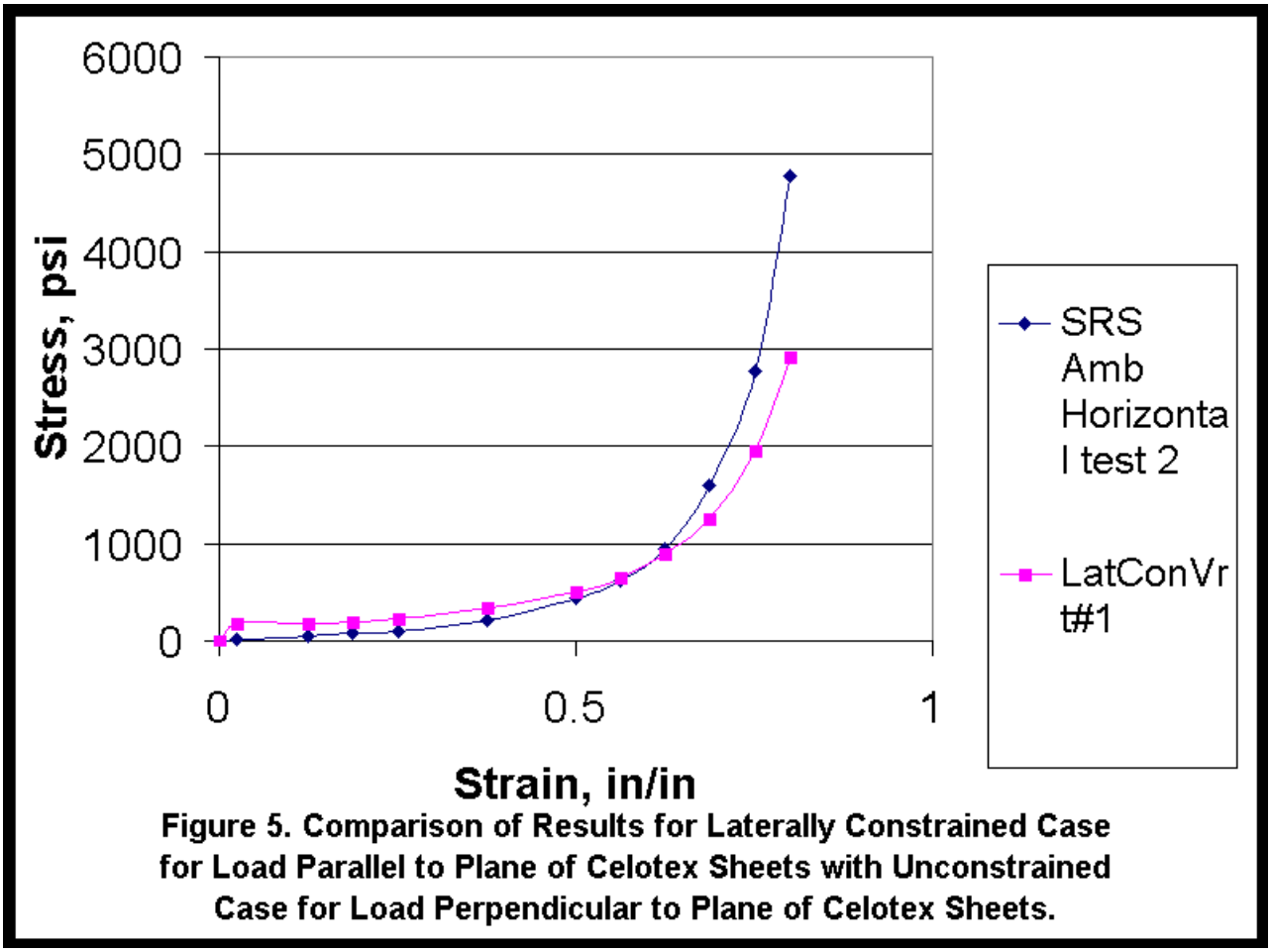

Figure 5. Comparison of Results for Laterally Constrained Case for Load Parallel to Plane of Celotex Sheets with Unconstrained Case for Load Perpendicular to Plane of Celotex Sheets.

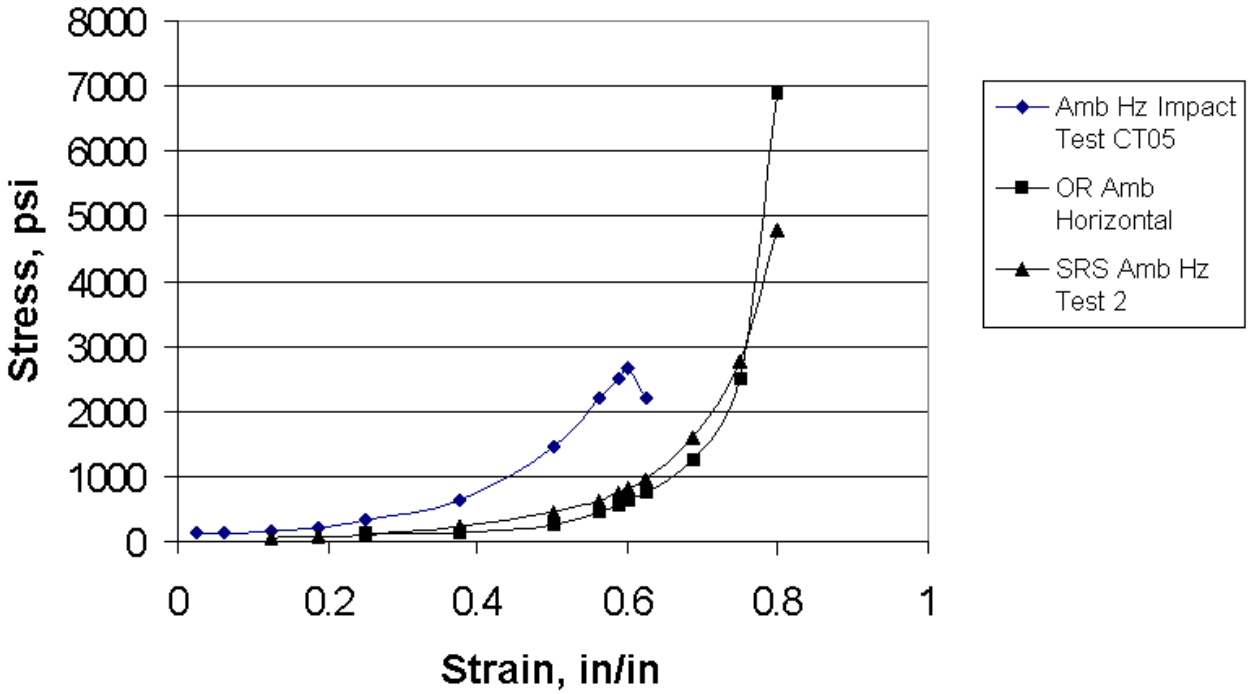

Figure 6. Comparison of Impact and Slow-Strain Response for Loading Perpendicular to the Plane of the Celotex Sheets

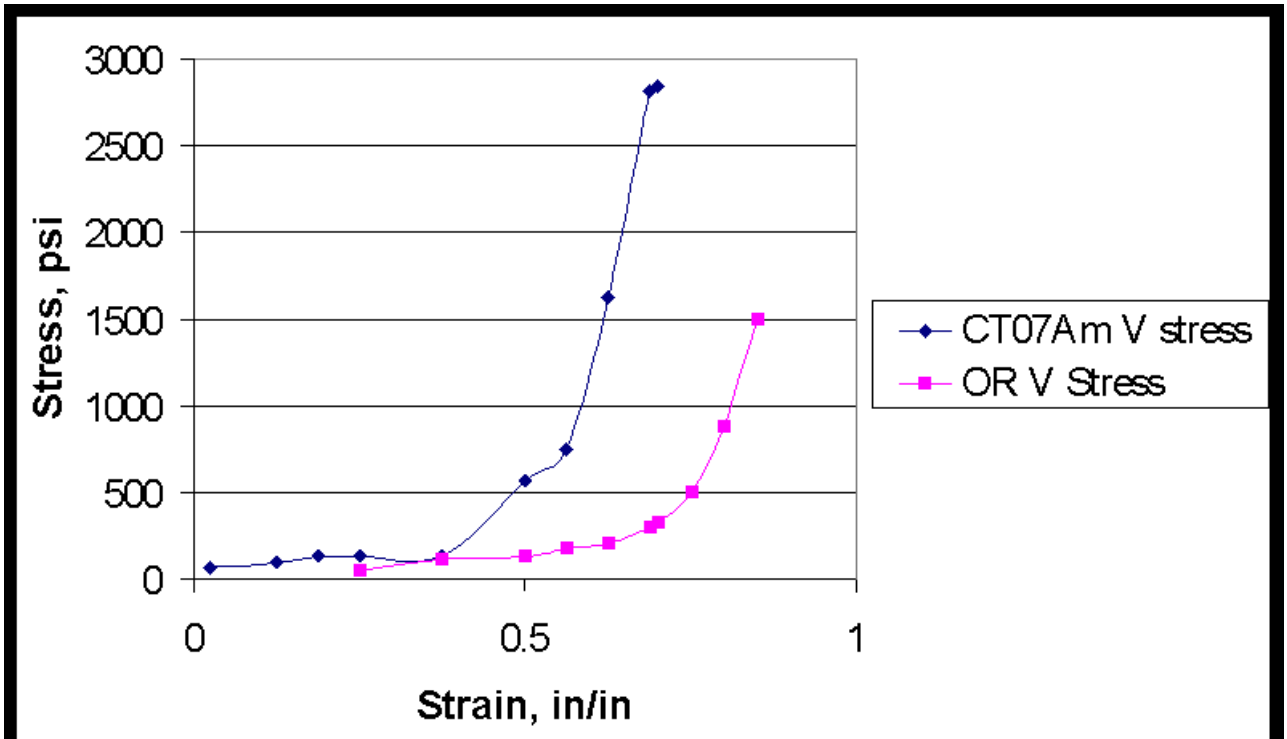

Figure 7. Comparison of Impact and Slow Strain-Rate Response for Loading Parallel to Plane of Celotex Sheets.

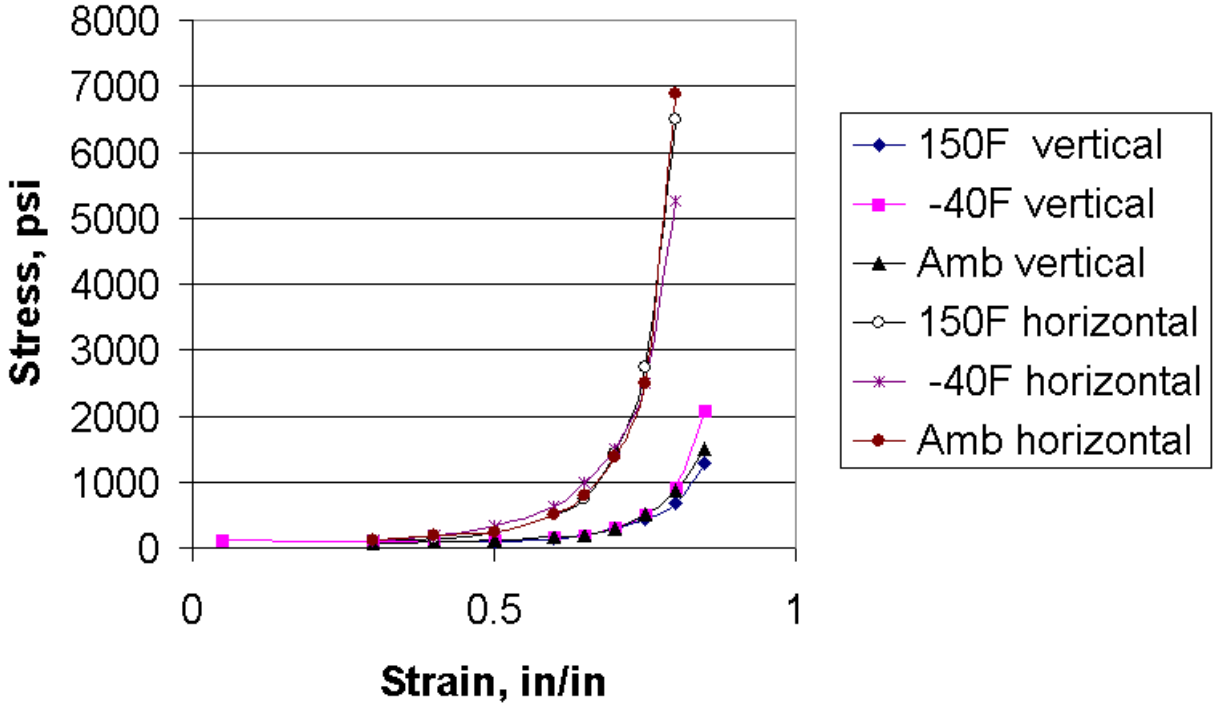

Figure 8. Oak Ridge Data Comparison

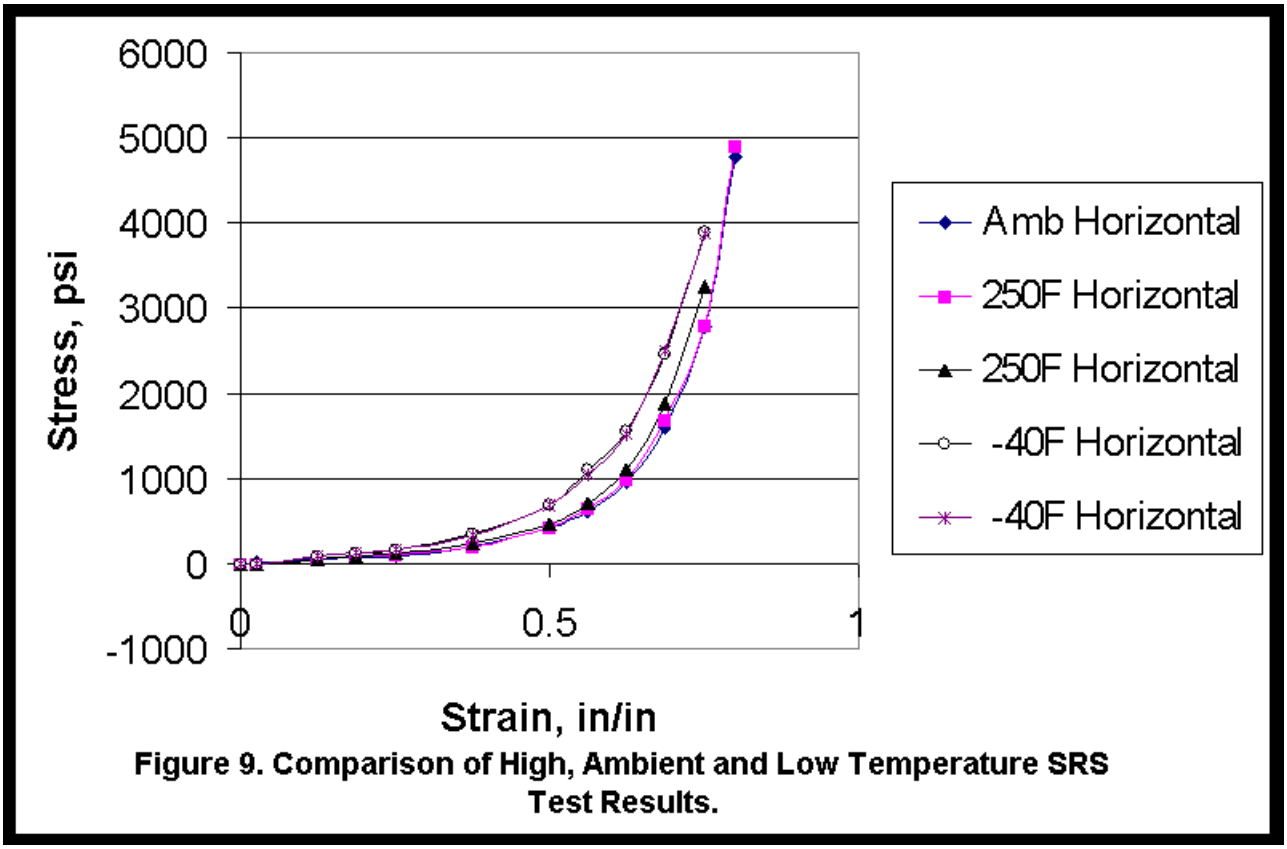

Figure 9. Comparison of High, Ambient and Low Temperature SRS Test Results.

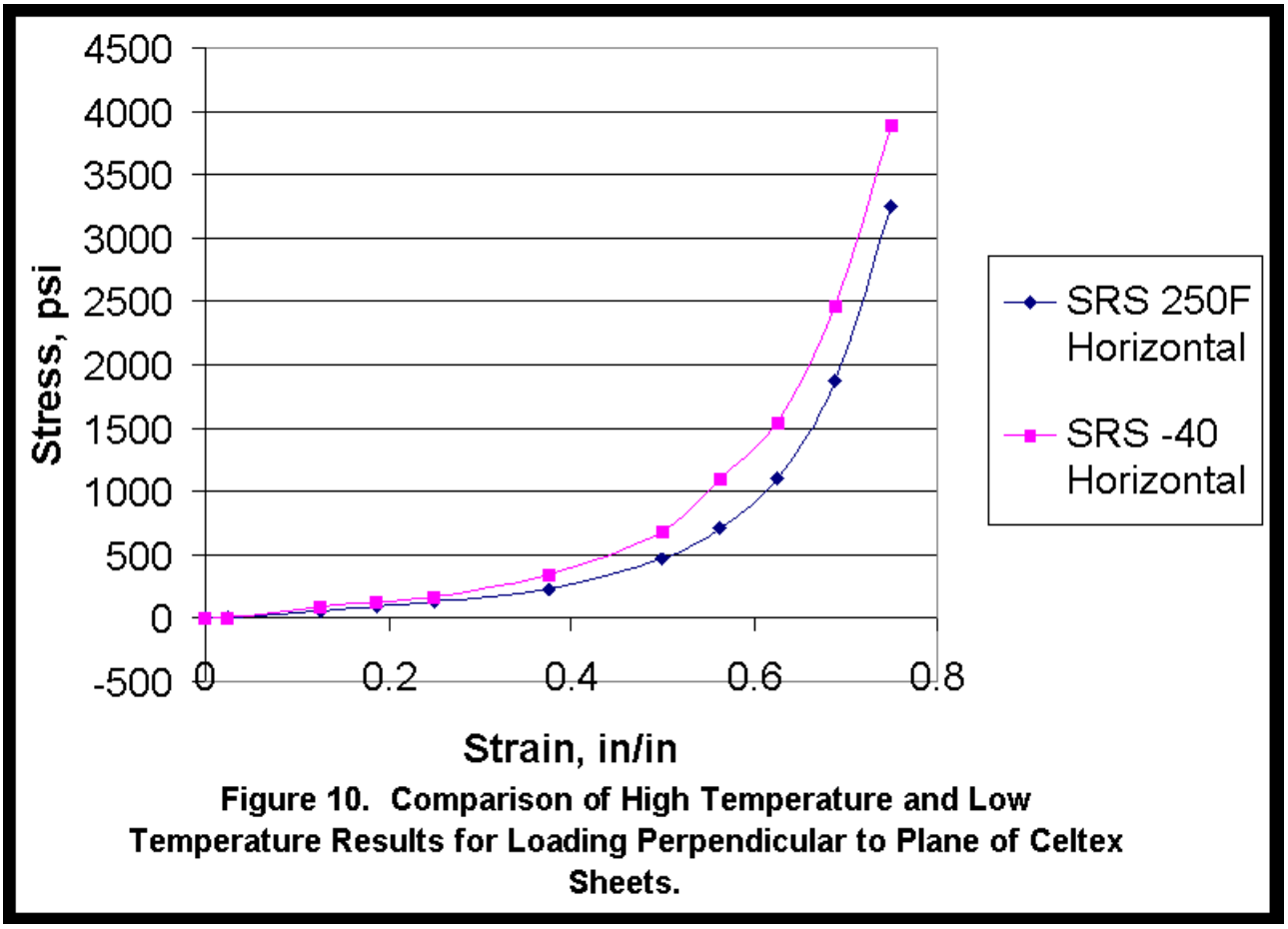

Figure 10. Comparison of High Temperature and Low Temperature Results for Loading Perpendicular to Plane of Celtex Sheets.

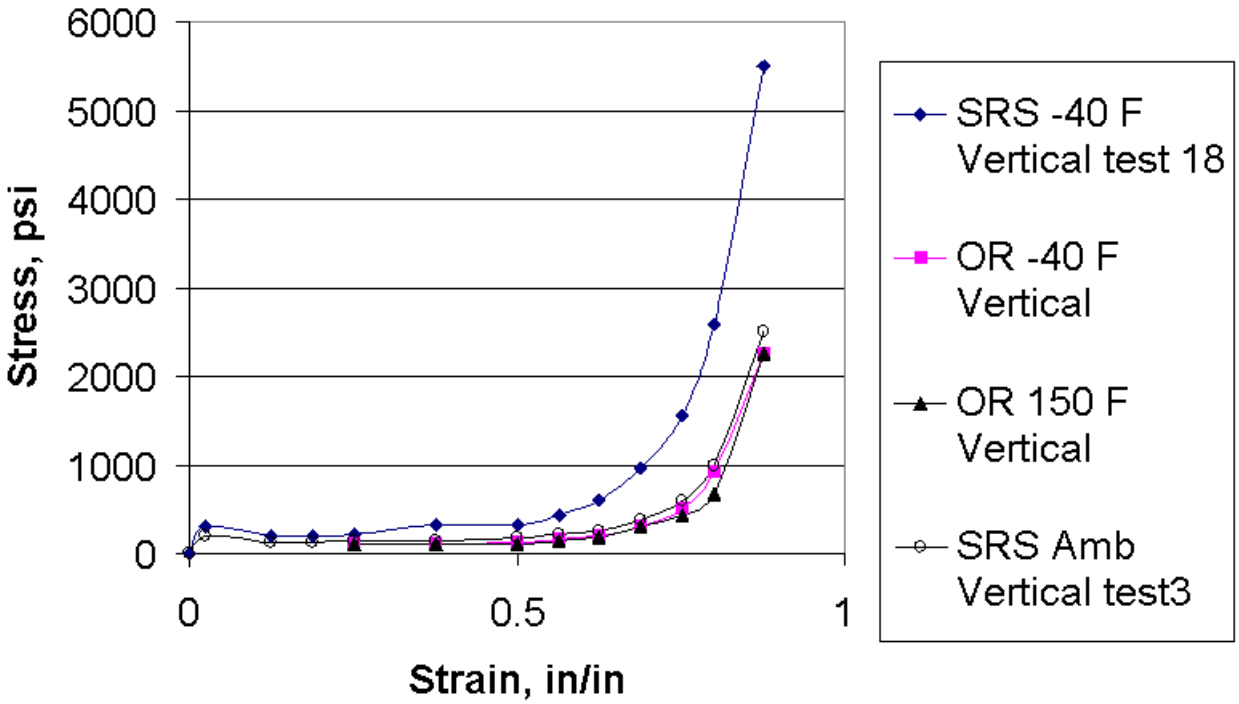

Figure 11. Comparison of High, Ambient and Low Temperature Results for Loading Parallel to Plane of Celotex Sheets.

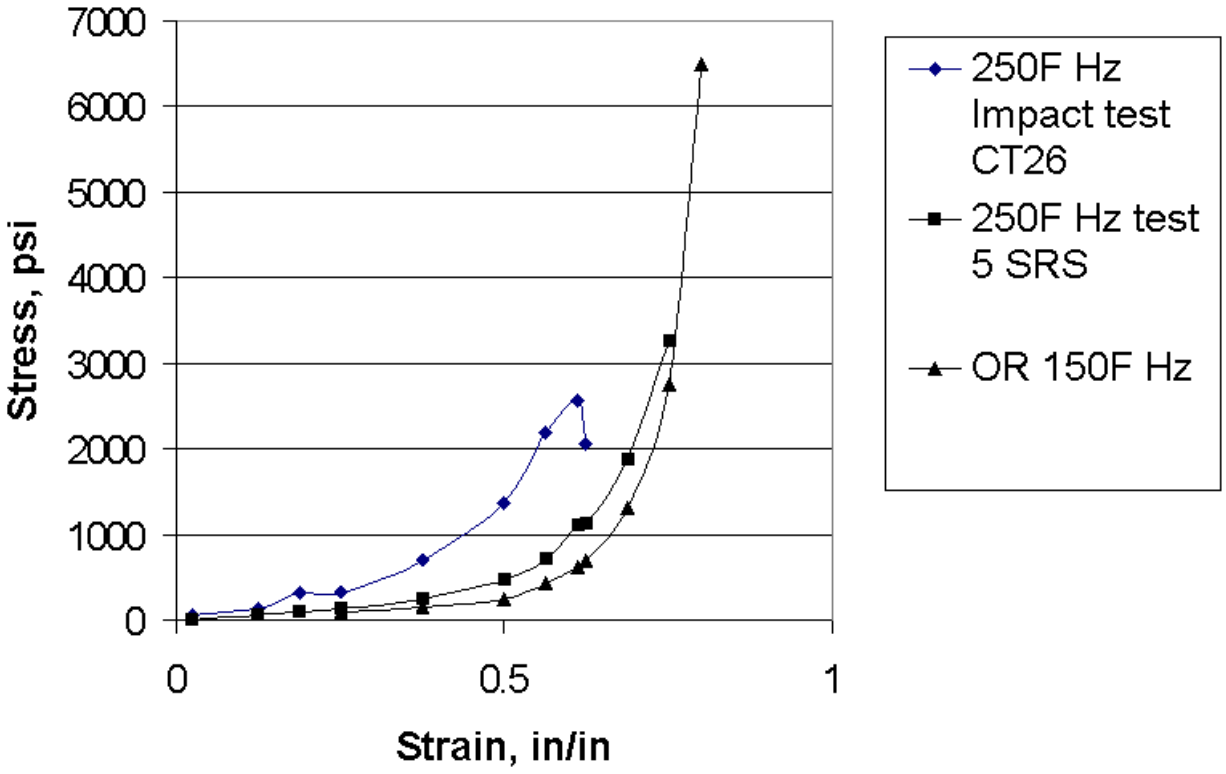

Figure 12. Comparison of Impact and Slow Strain Results at High Temperature for Load Perpendicular to Plane of Celotex Sheets

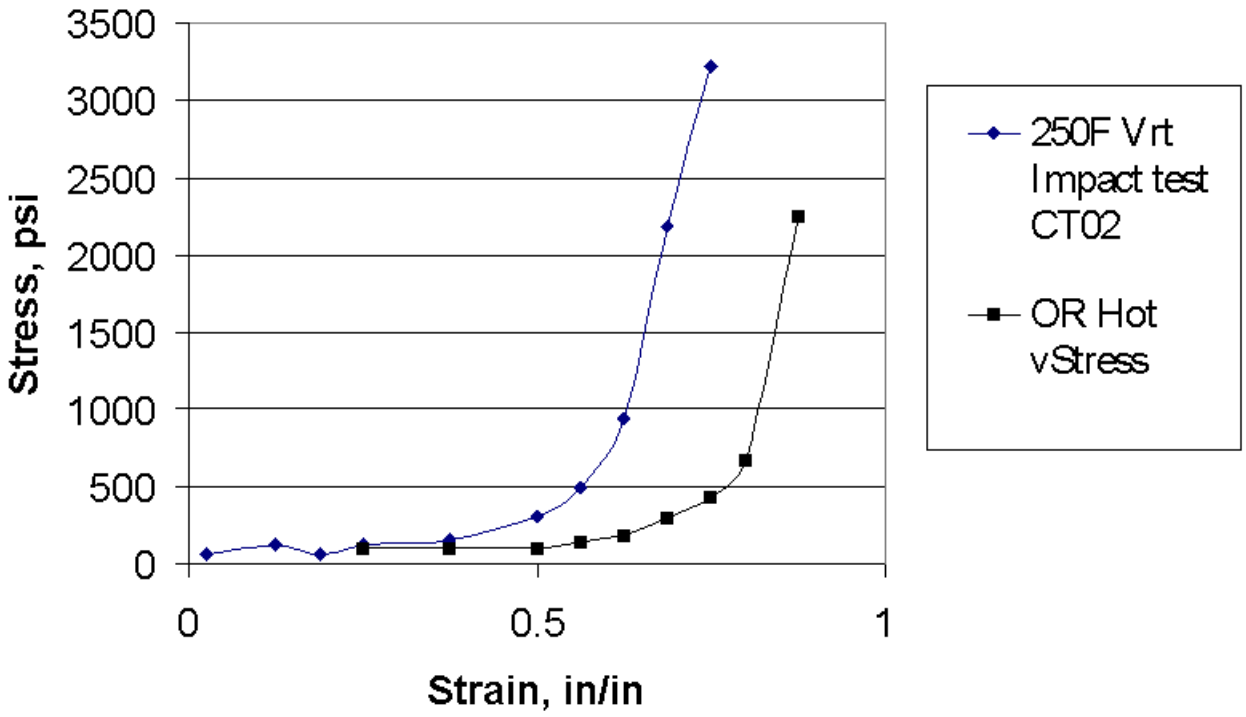

Figure 13. Comparison of Impact and Slow Strain Results at High Temperature for Load Parallel to Plane of Celotex Sheets.

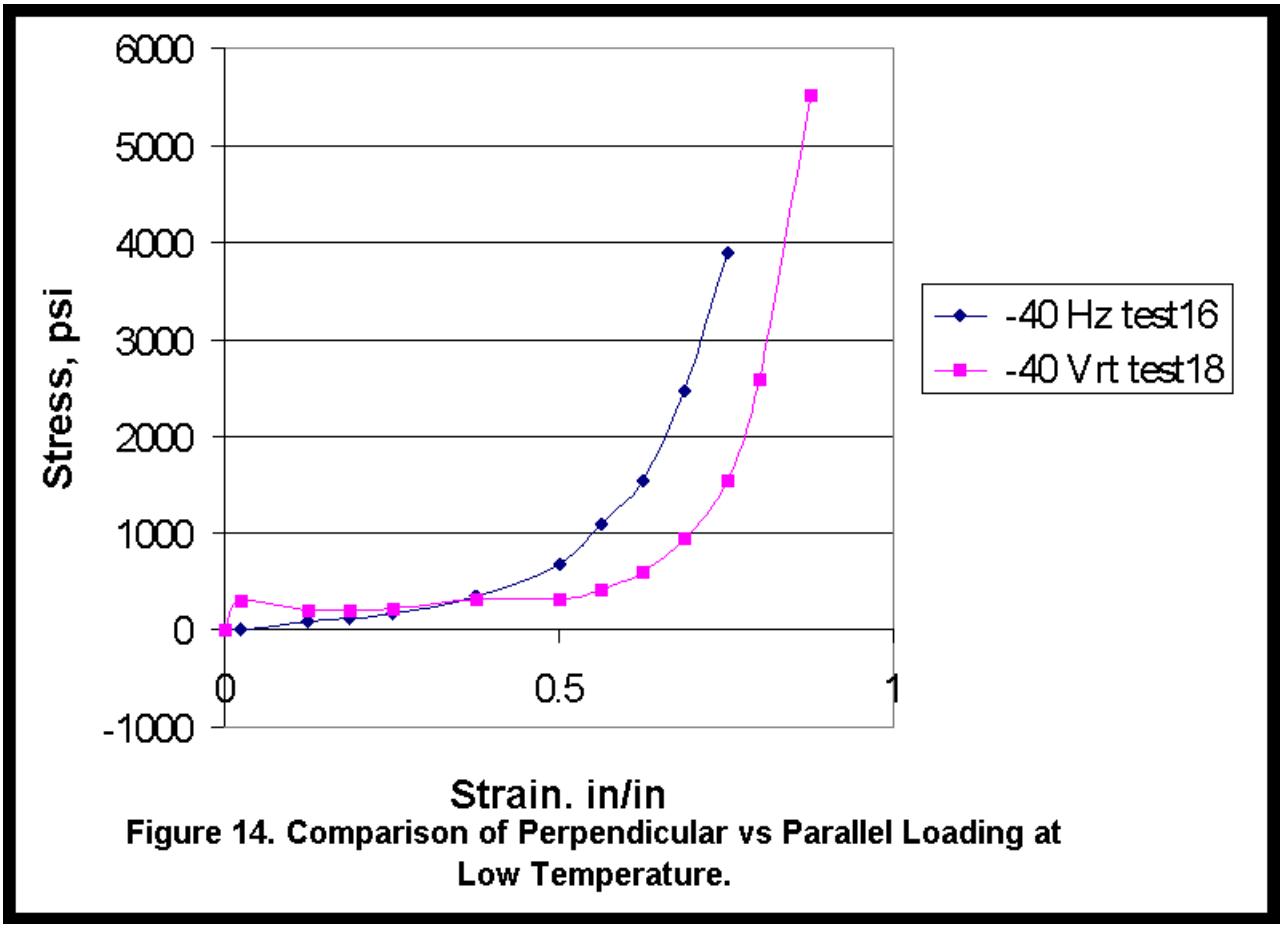

Figure 14. Comparison of Perpendicular vs Parallel Loading at Low Temperature.

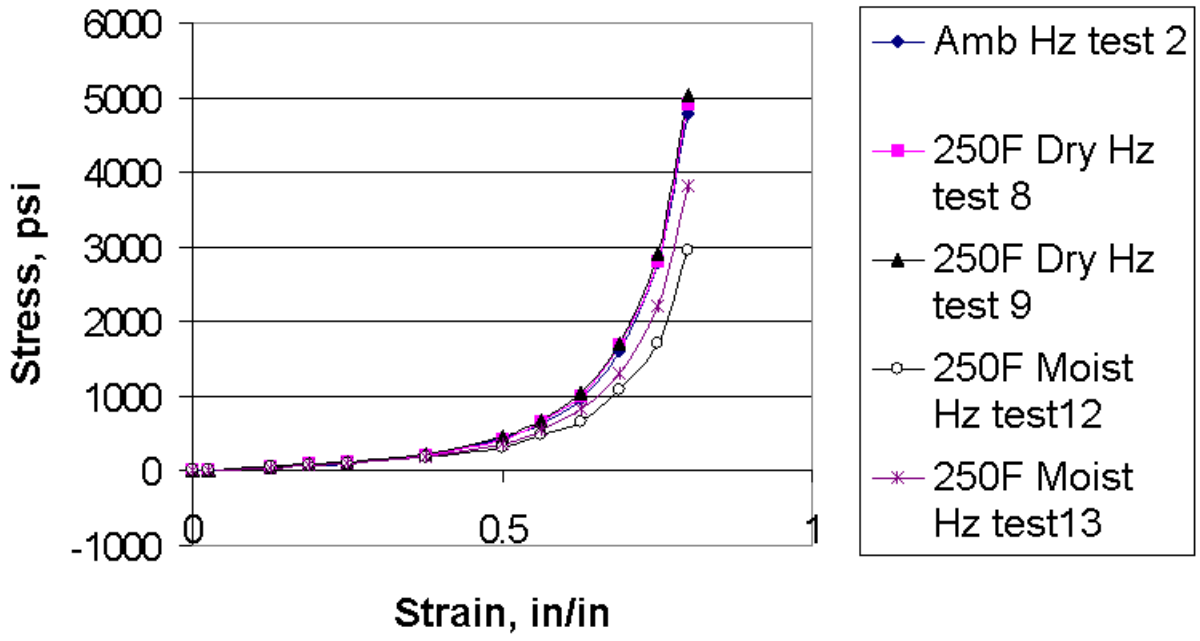

Figure 15. Comparison of Hot Dry and Hot Humidified Results for SRS Specimens for Load Perpendicular to Plane of Celotex Sheets.

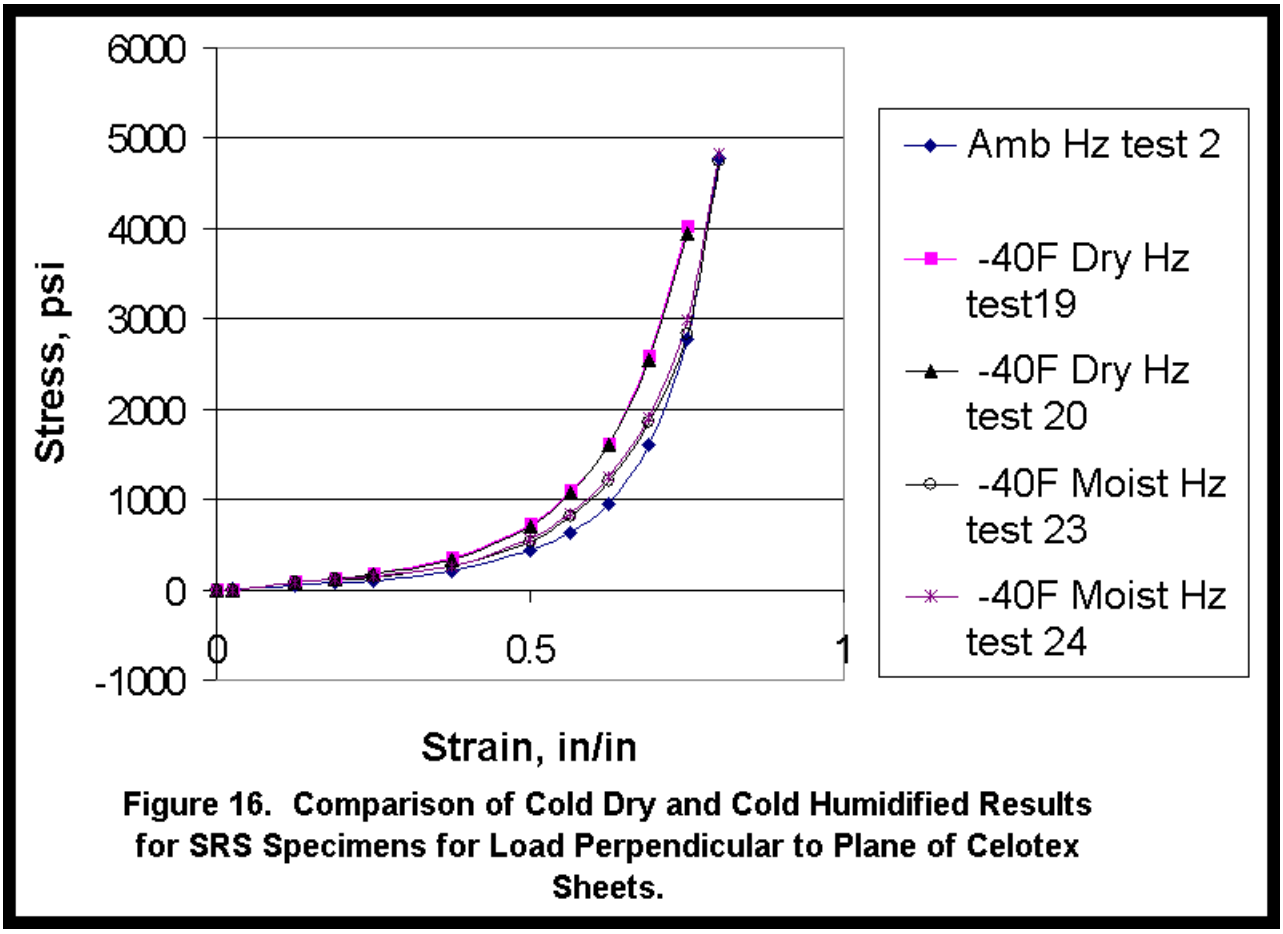

Figure 16. Comparison of Cold Dry and Cold Humidified Results for SRS Specimens for Load Perpendicular to Plane of Celotex Sheets.

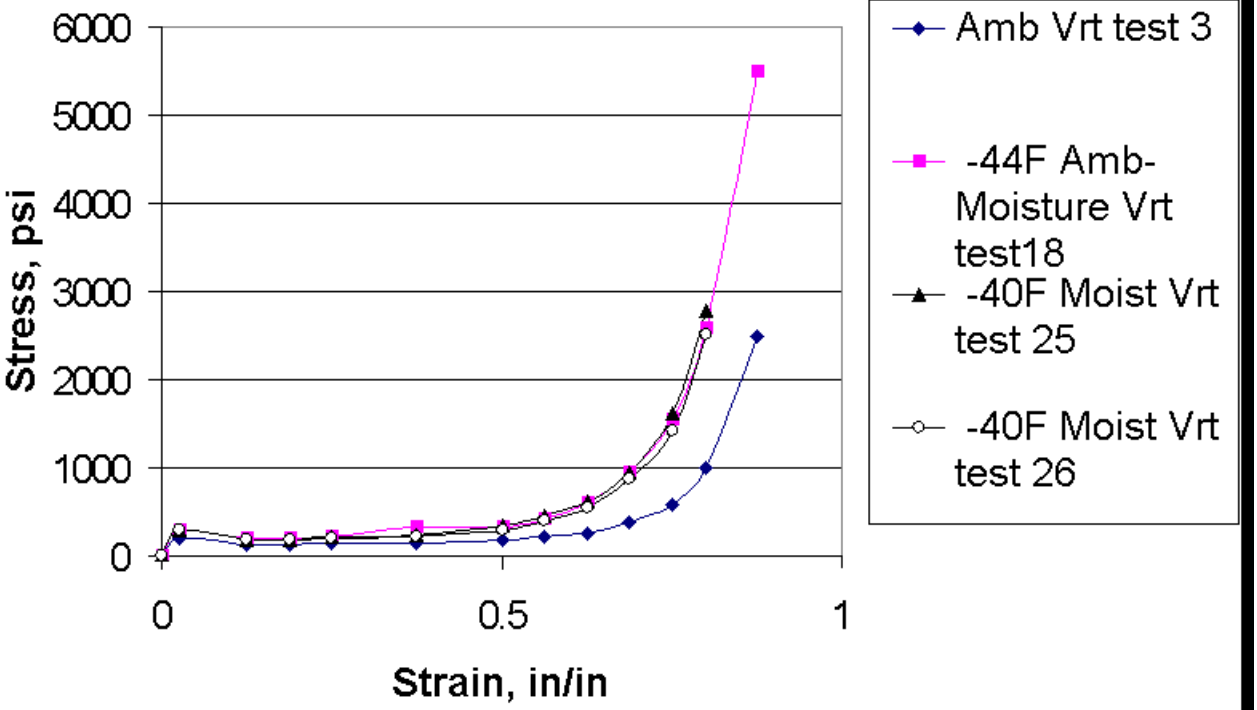

Figure 17. Comparison of Cold Ambient and Cold Humidified Results for Loading Parallel to Plane of Celotex Sheets.

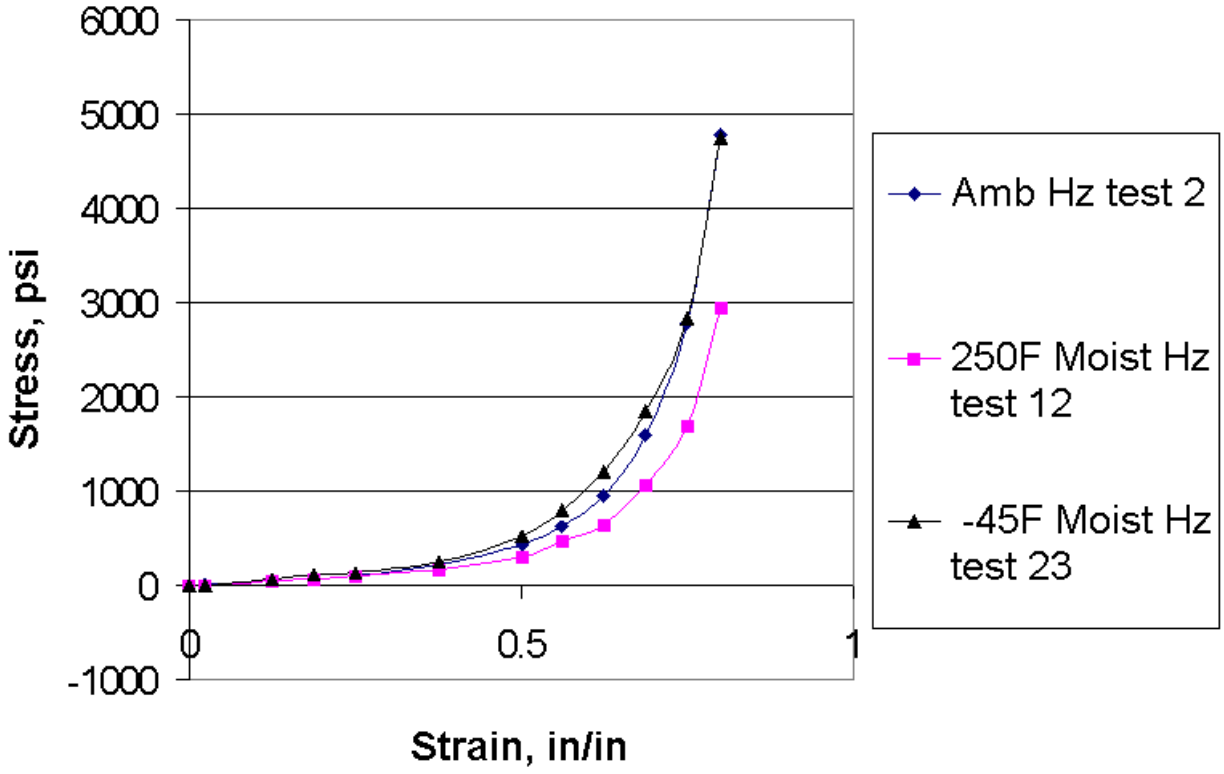

Figure 18. Comparison of Hot Moist and Cold Moist Results with Load Perpendicular to Plane of Celotex Sheets.

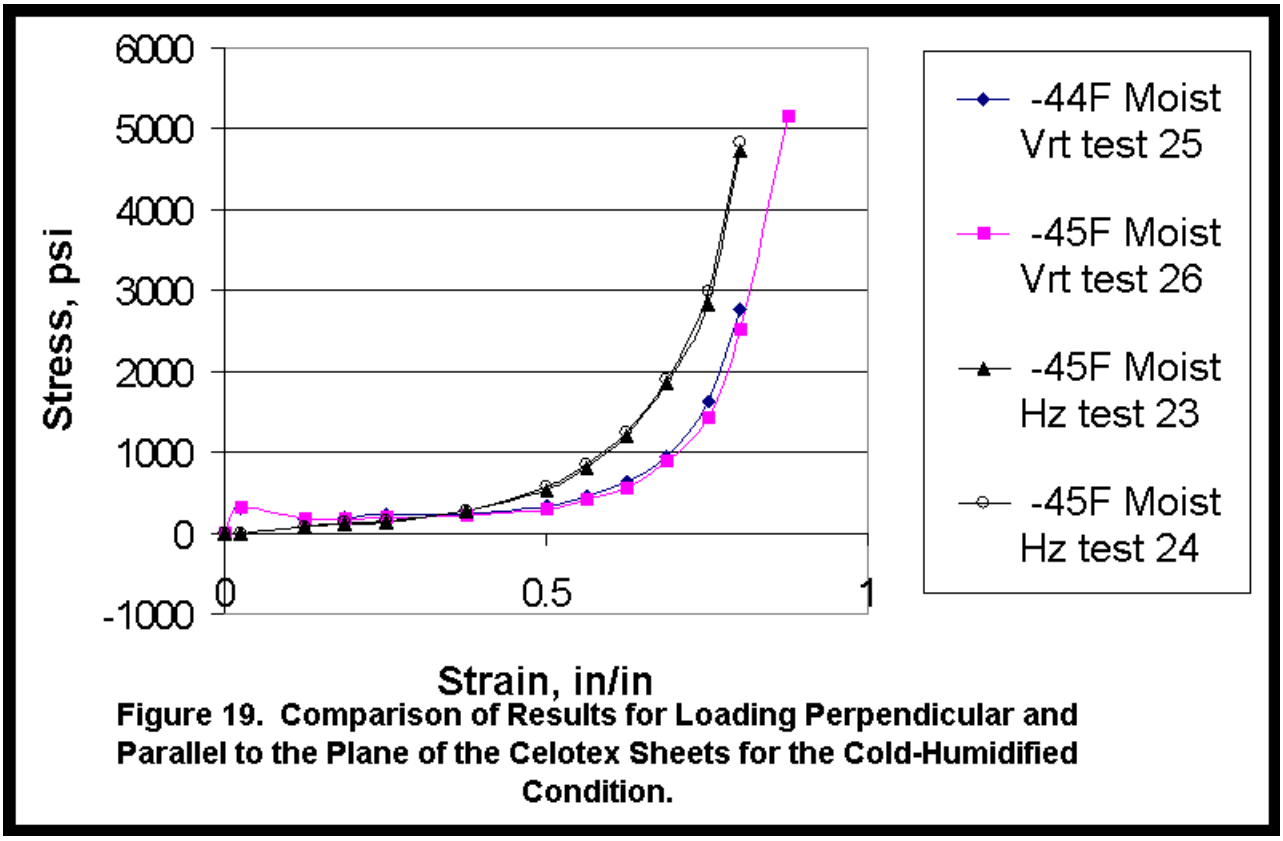

Figure 19. Comparison of Results for Loading Perpendicular and Parallel to the Plane of the Celotex Sheets for the Cold-Humidified Condition.

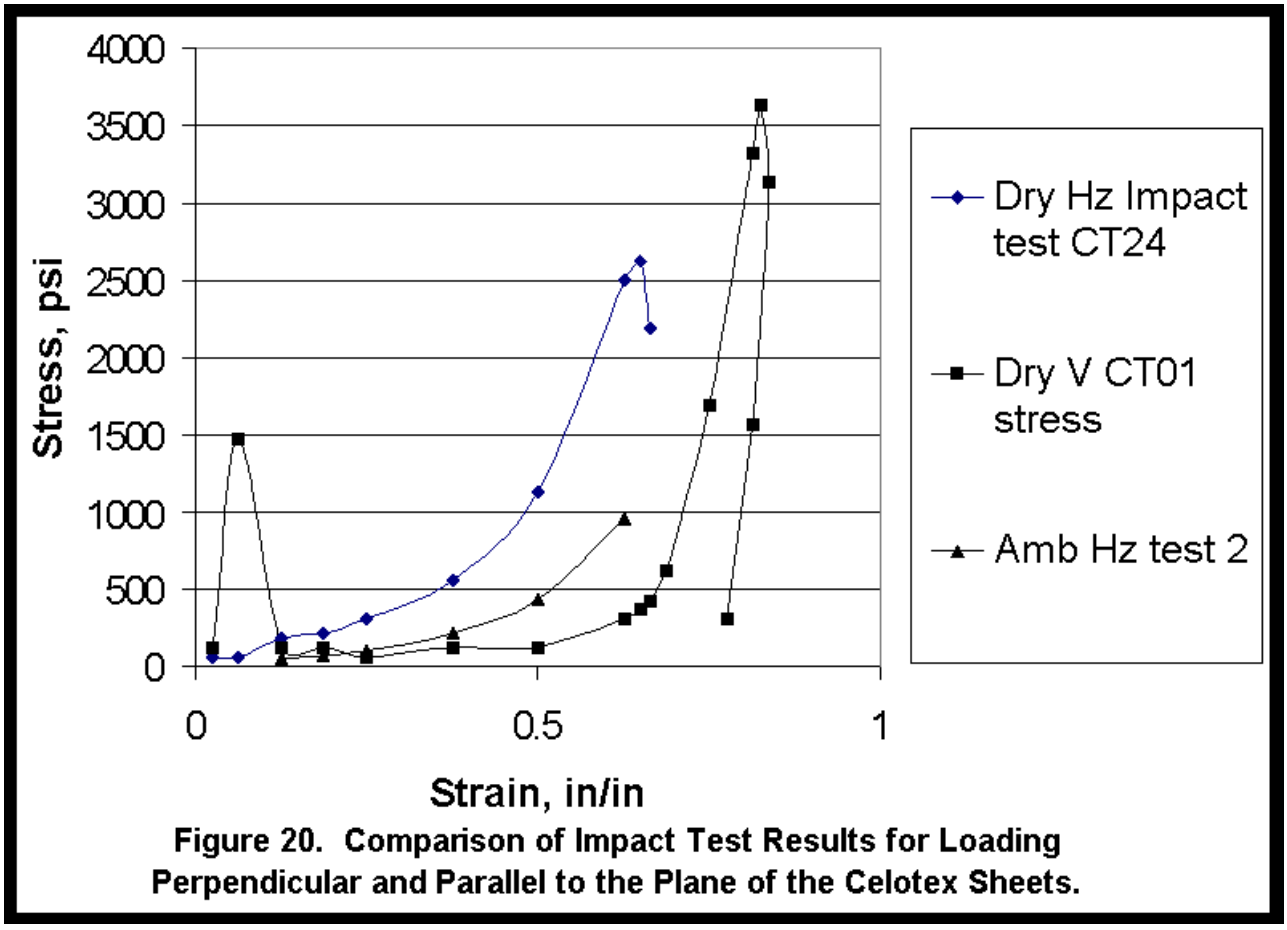

Figure 20. Comparison of Impact Test Results for Loading Perpendicular and Parallel to the Plane of the Celotex Sheets.

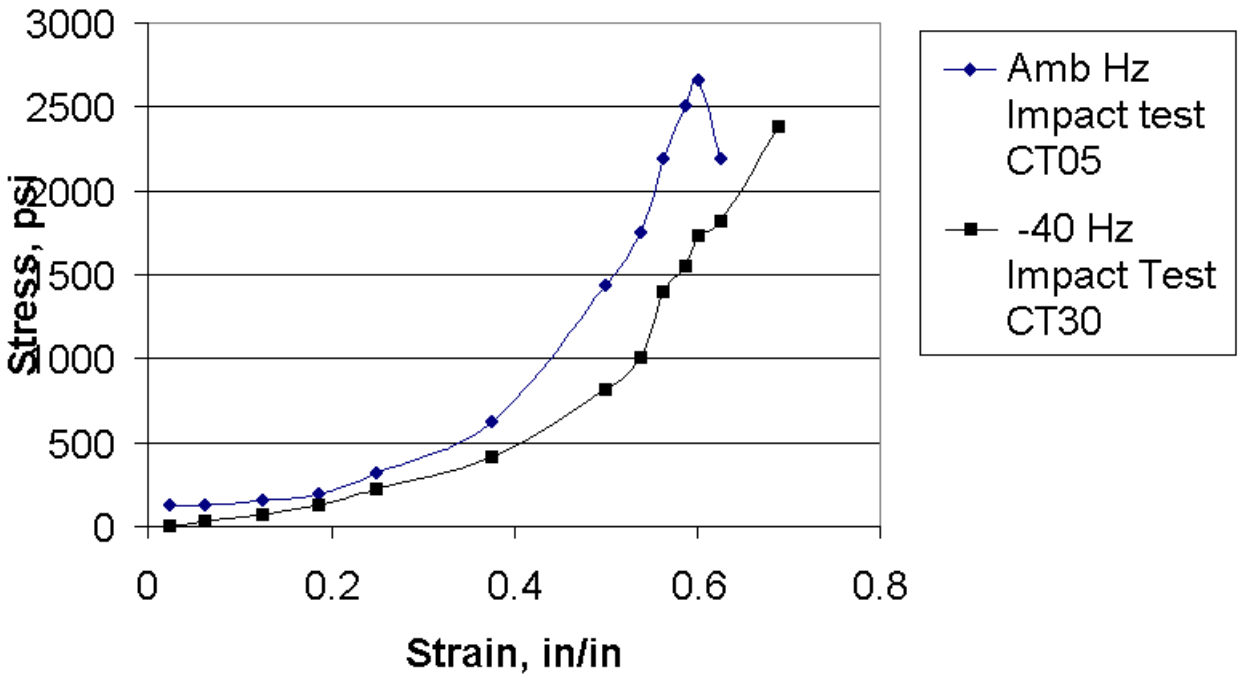

Figure 21. Comparison of Ambient and Cold Impact Results for Loading Perpendicular to the Plane of the Celotex Sheets.

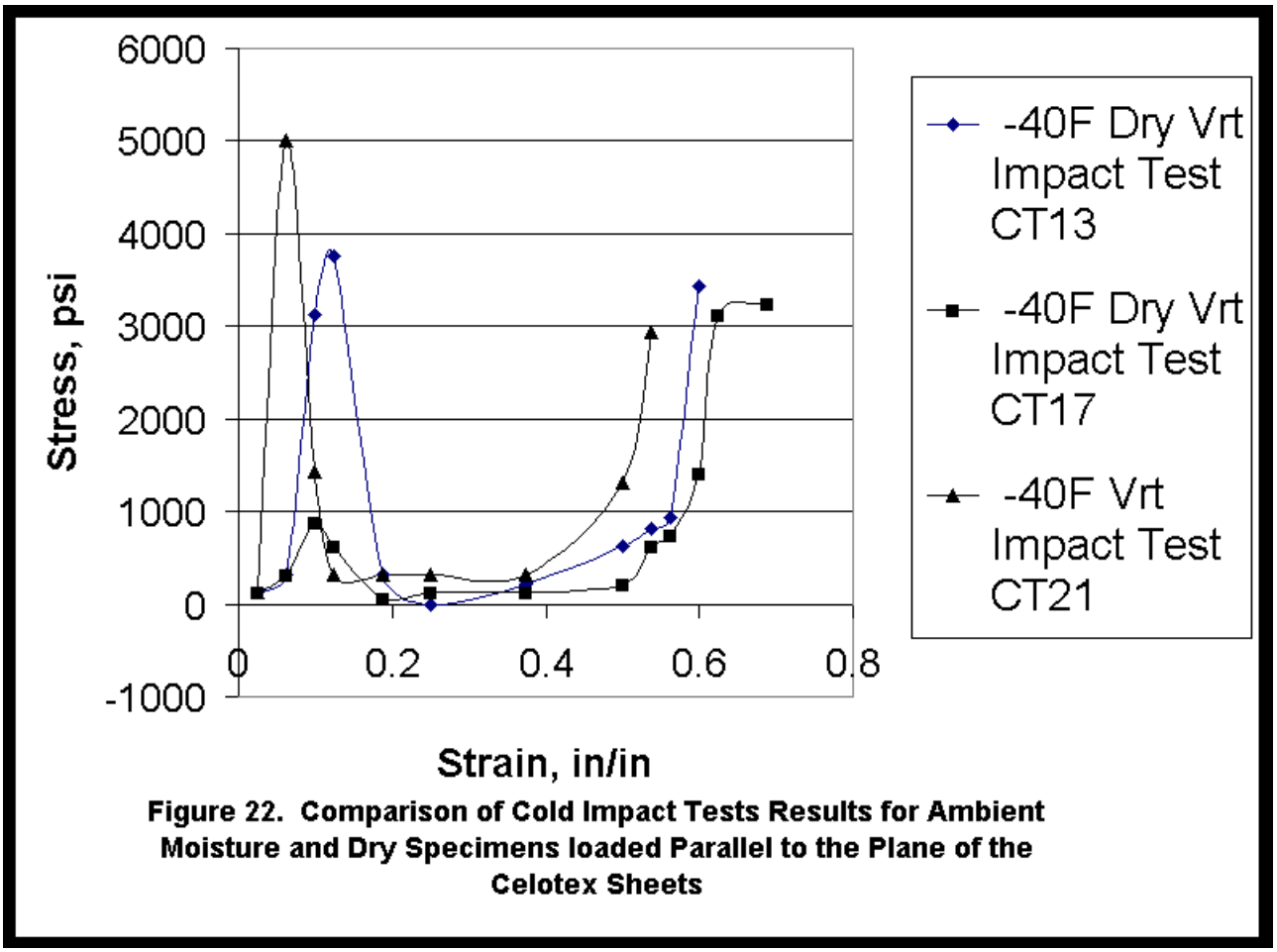

Figure 22. Comparison of Cold Impact Tests Results for Ambient Moisture and Dry Specimens loaded Parallel to the Plane of the Celotex Sheets

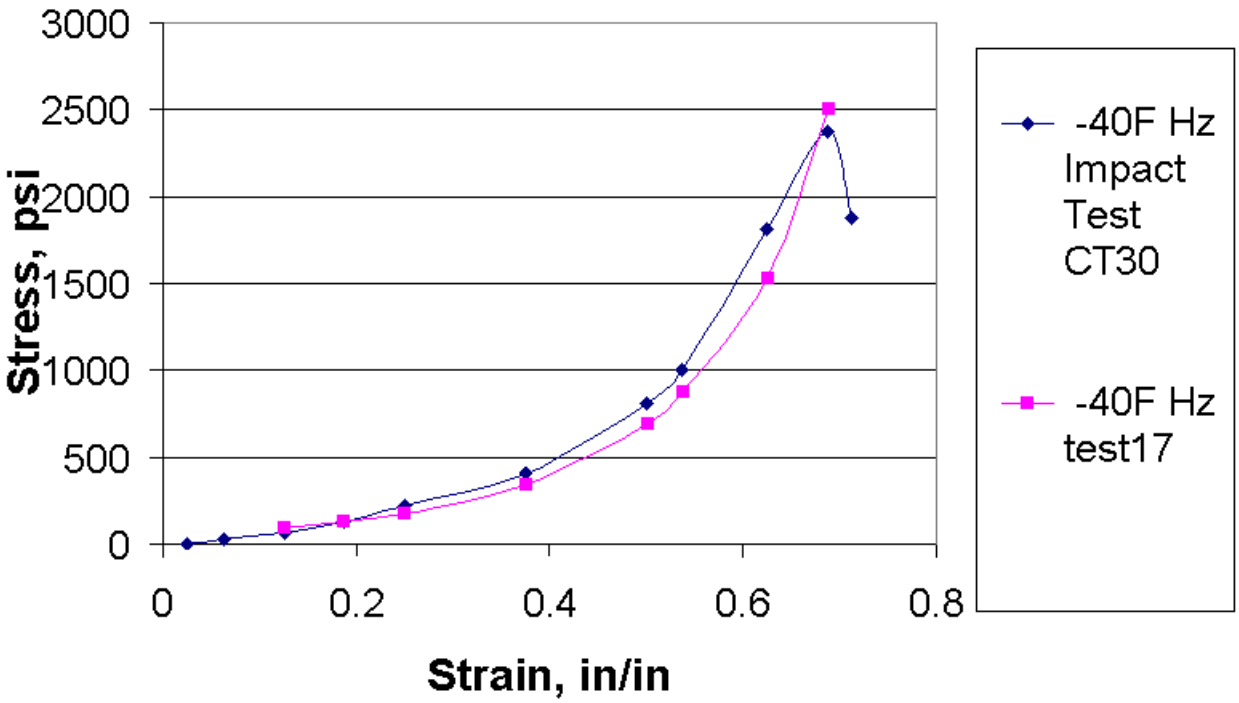

Figure 23. Comparison of Cold Impact Test Results with Cold Slow Strain-Rate Test Results for Load Perpendicular to Sheets.

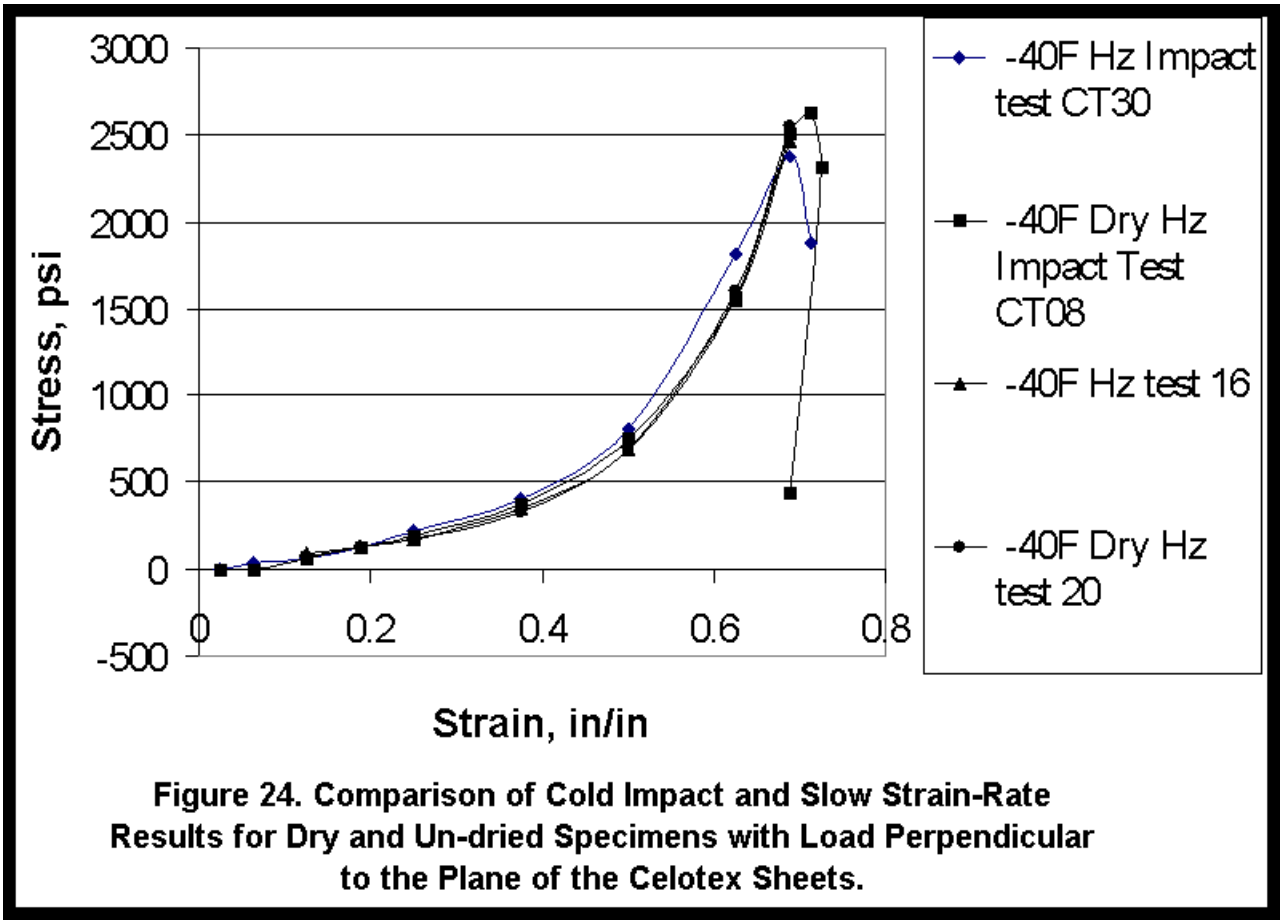

Figure 24. Comparison of Cold Impact and Slow Strain-Rate Results for Dry and Un-dried Specimens with Load Perpendicular to the Plane of the Celotex Sheets.

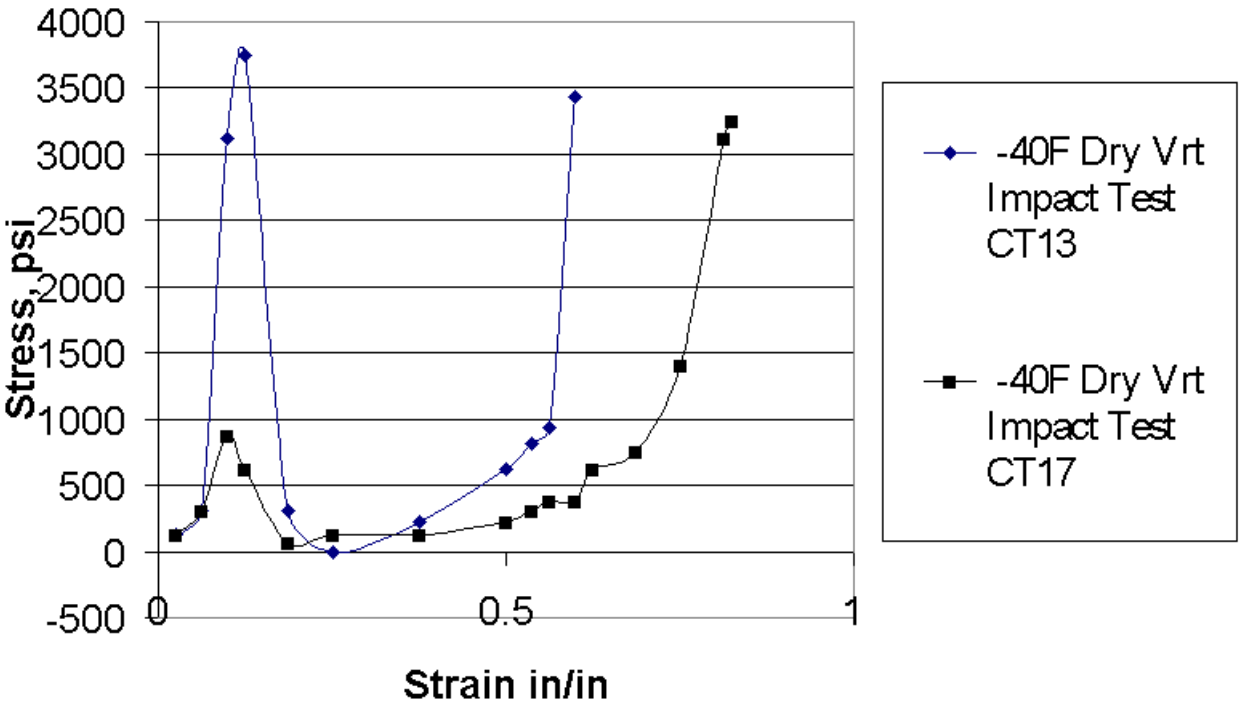

Figure 25. Results of Cold, Dry Impact Tests with Load Parallel to the Plane of the Celotex Sheets.

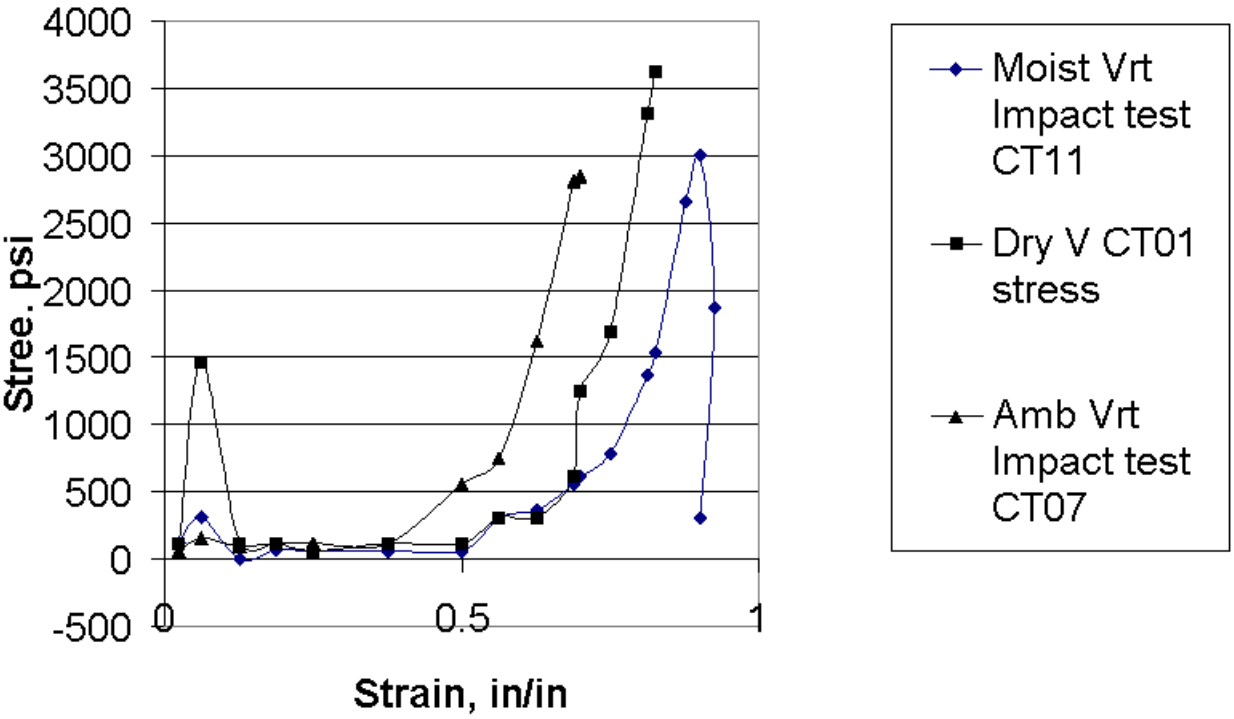

Figure 26. Comparison of Moist, Dry and Ambient-Moisture Impact Test Results for Load Parallel to the Plane of the Celotex Sheets.

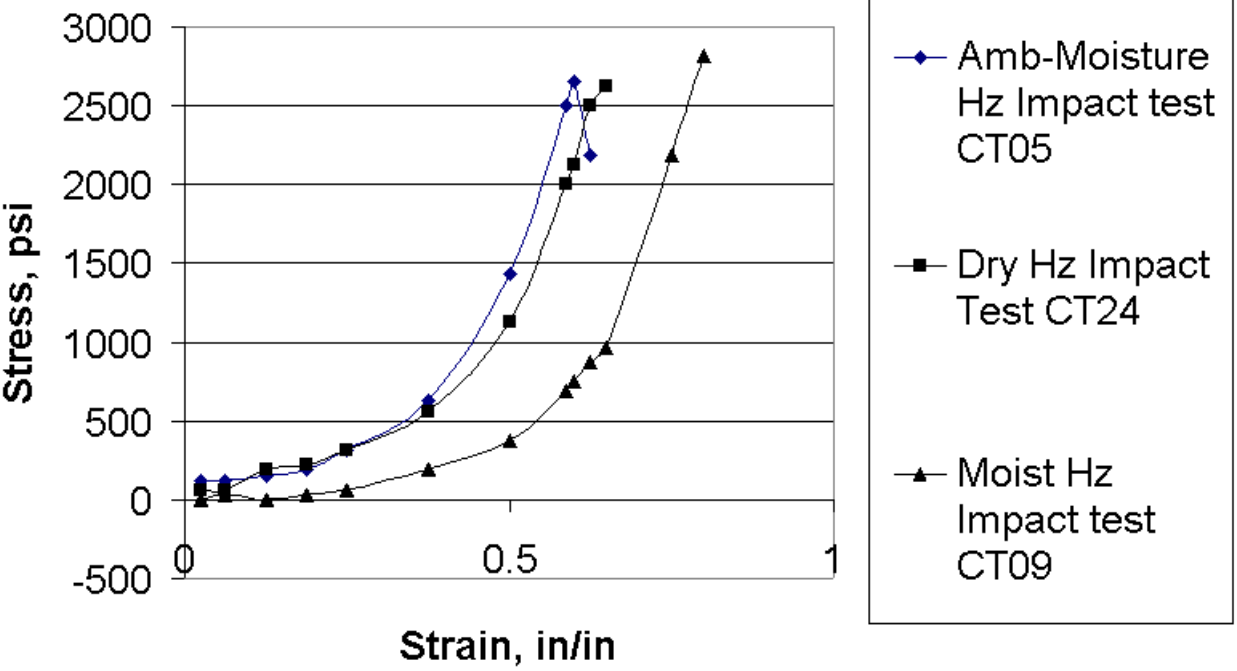

Figure 27. Comparison of Moist, Dry and Ambient Moisture Impact Test Results for Load Perpendicular to the Plane of the Celotex Sheets.

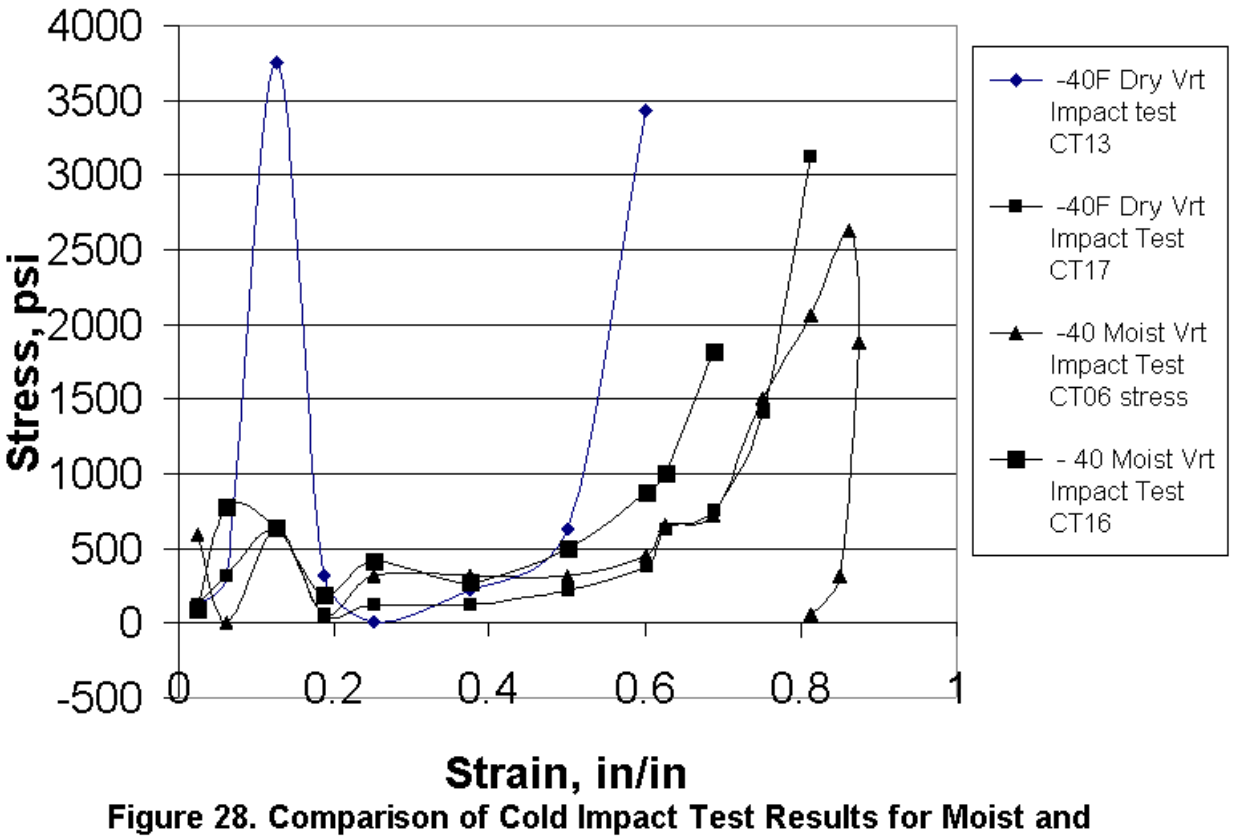

Figure 28. Comparison of Cold Impact Test Results for Moist and Dry Specimens Loaded Parallel to the Plane of the Celotex

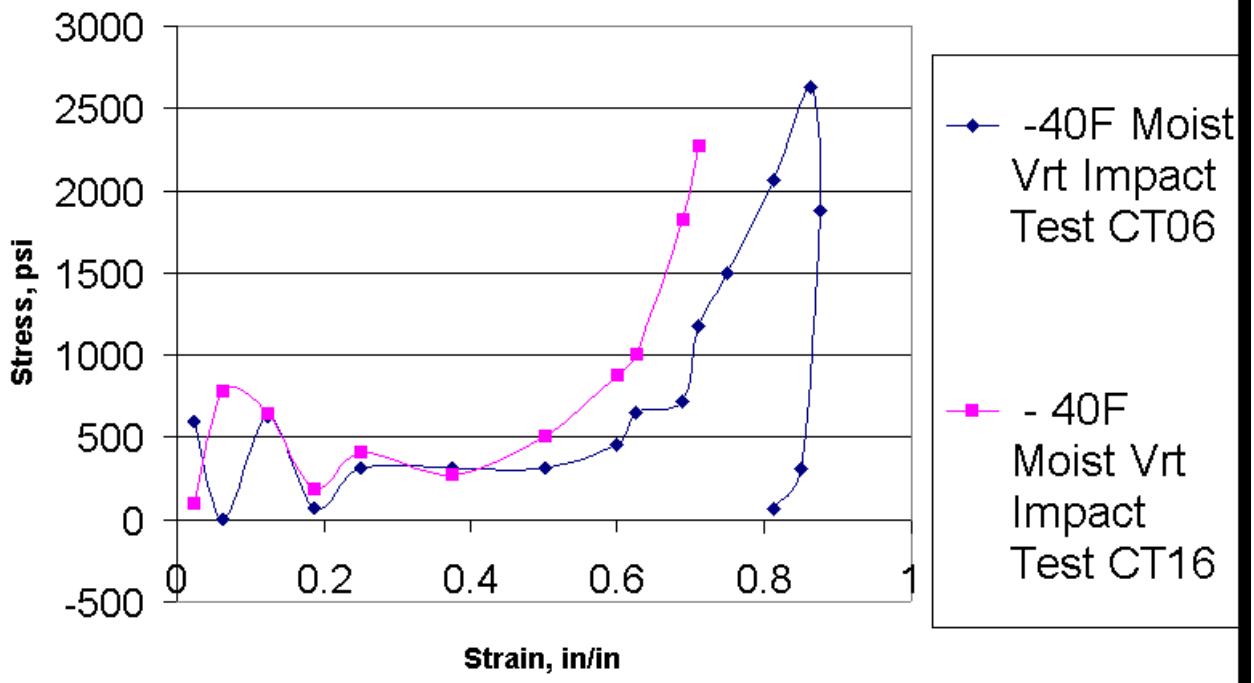

Figure 29. Cold Moist Impact Test Results for Loading Parallel to Plane of Celotex Sheets

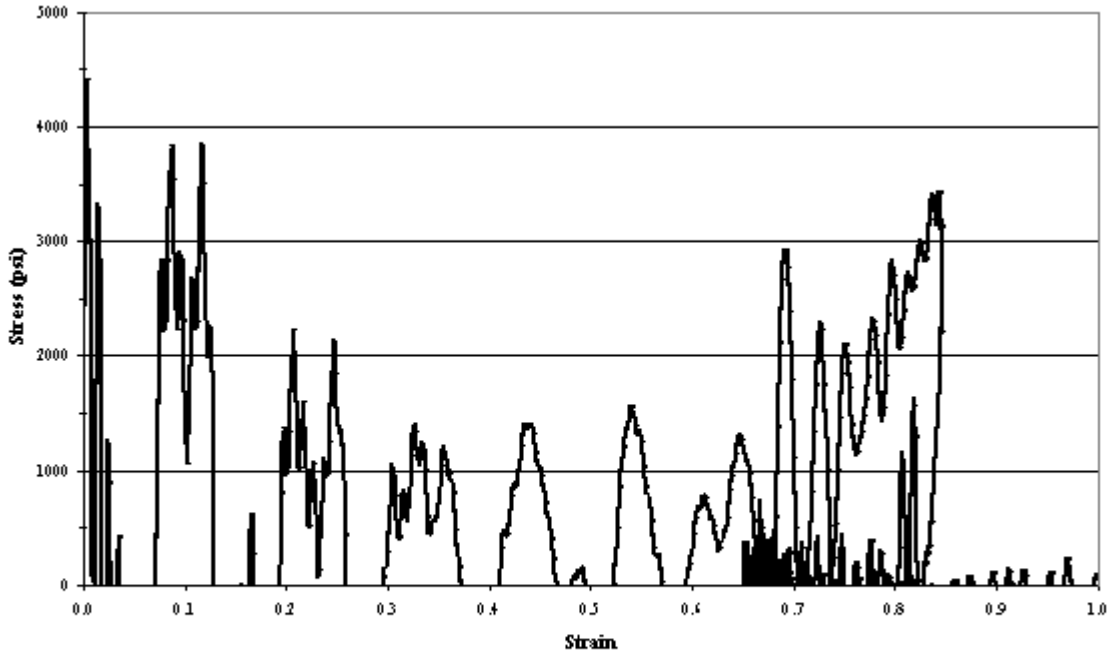

Figure 30. Second Series Impact Test Results for –40°F Specimen CTV with Load Parallel to Plane of Celotex Sheets.

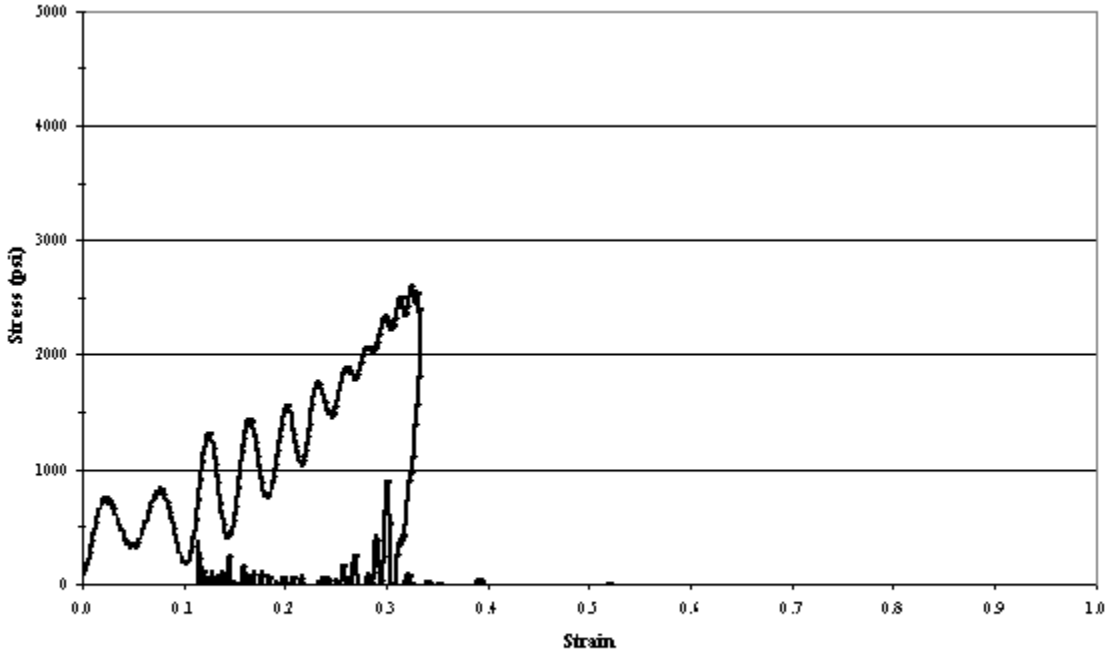

Figure 31. Second Series Impact Test Results for –40°F Specimen CT38 with Load Perpendicular to Plane of Celotex Sheets.

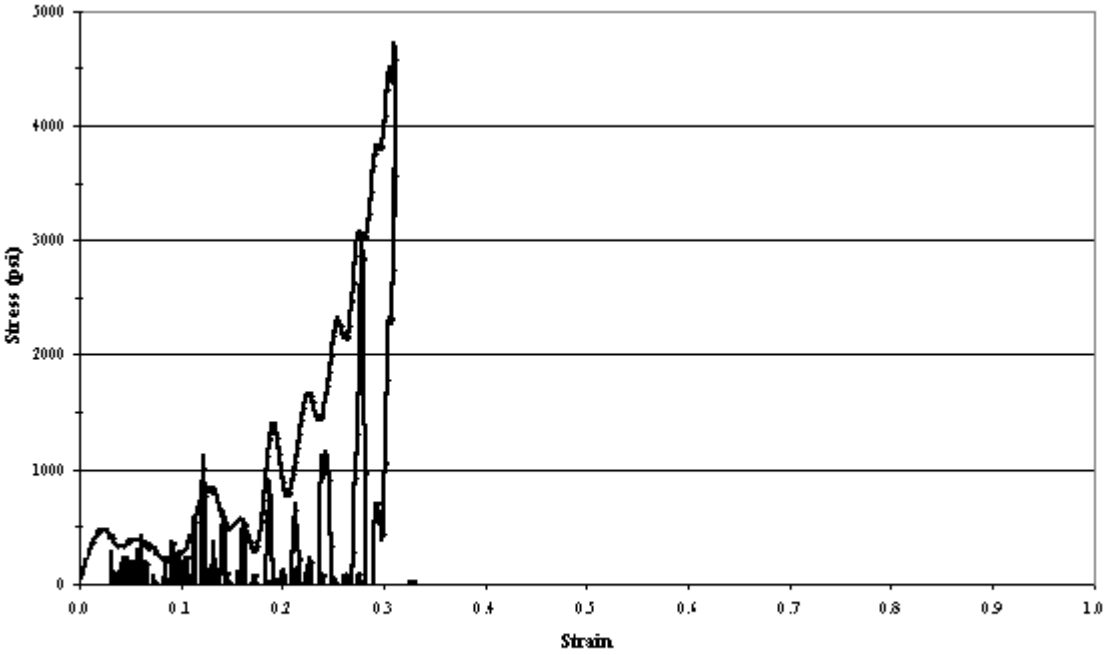

Figure 32. Second Series Impact Test Results for Hot Moist Specimen CT31 with Load Parallel to Plane of Celotex Sheets.

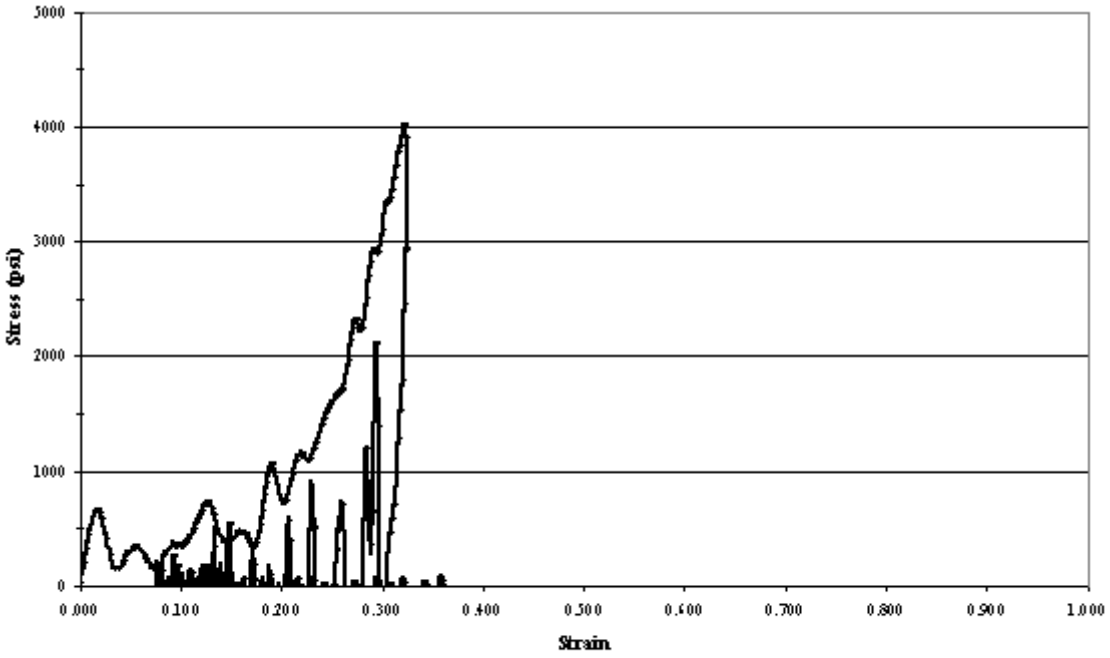

Figure 33. Second Series Impact Test Results for Hot Moist Specimen CT35 with Load Parallel to Plane of Celotex Sheets.

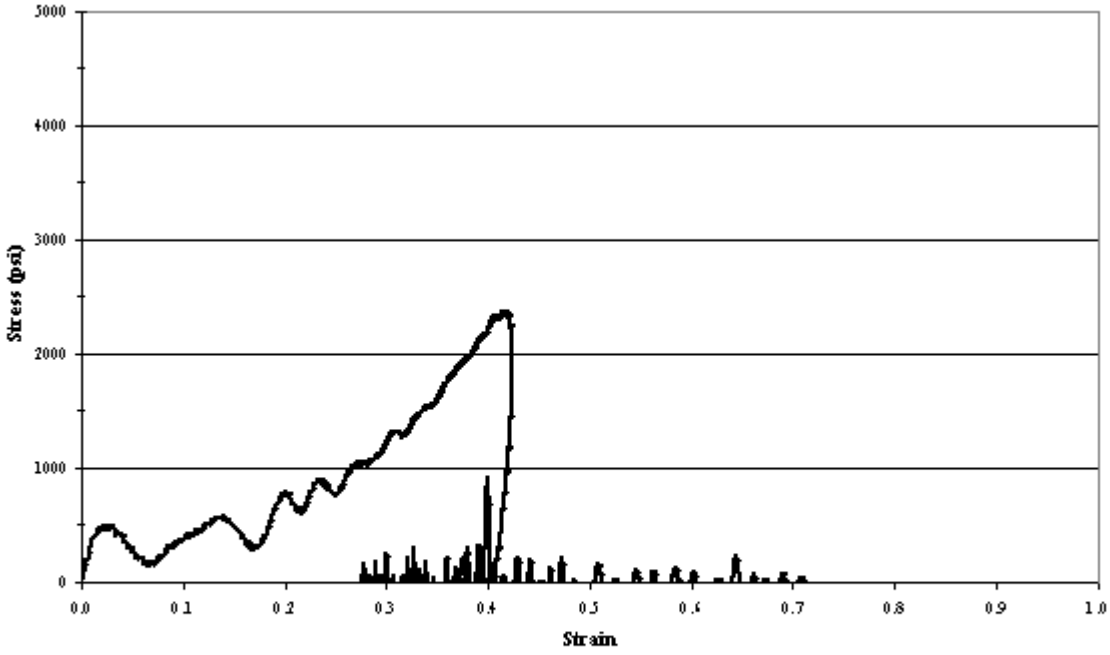

Figure 34. Second Series Impact Test Results for –40°F Moist Specimen CT14 with Load Perpendicular to Plane of Celotex Sheets.

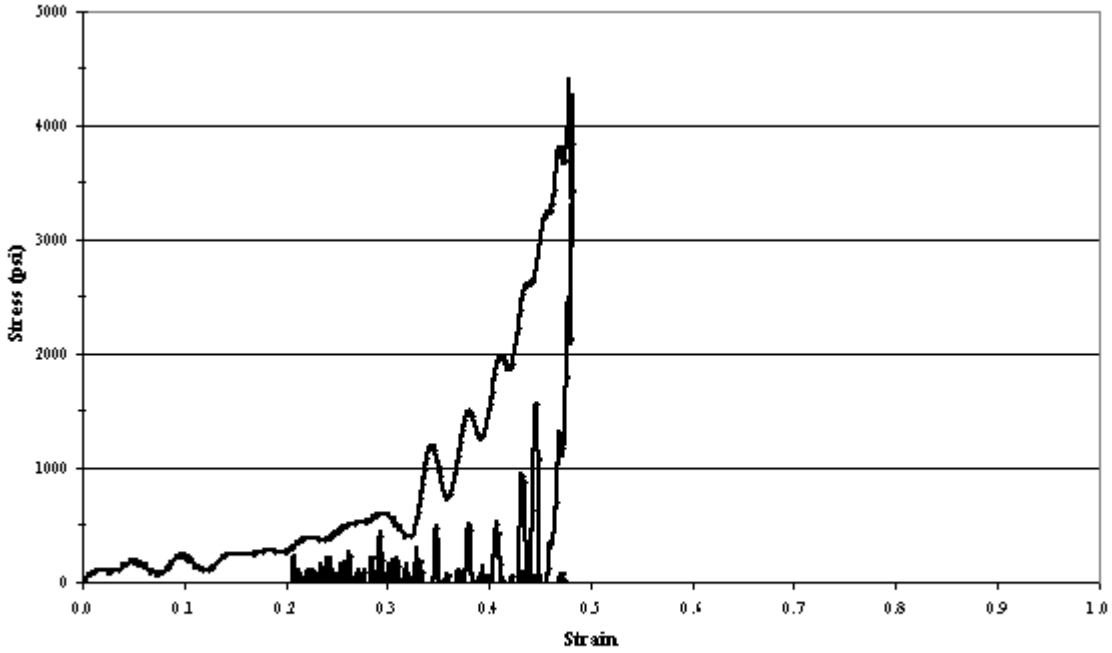

Figure 35. Second Series Impact Test Results for Hot Moist Specimen CT19 with Load Perpendicular to Plane of Celotex Sheets.

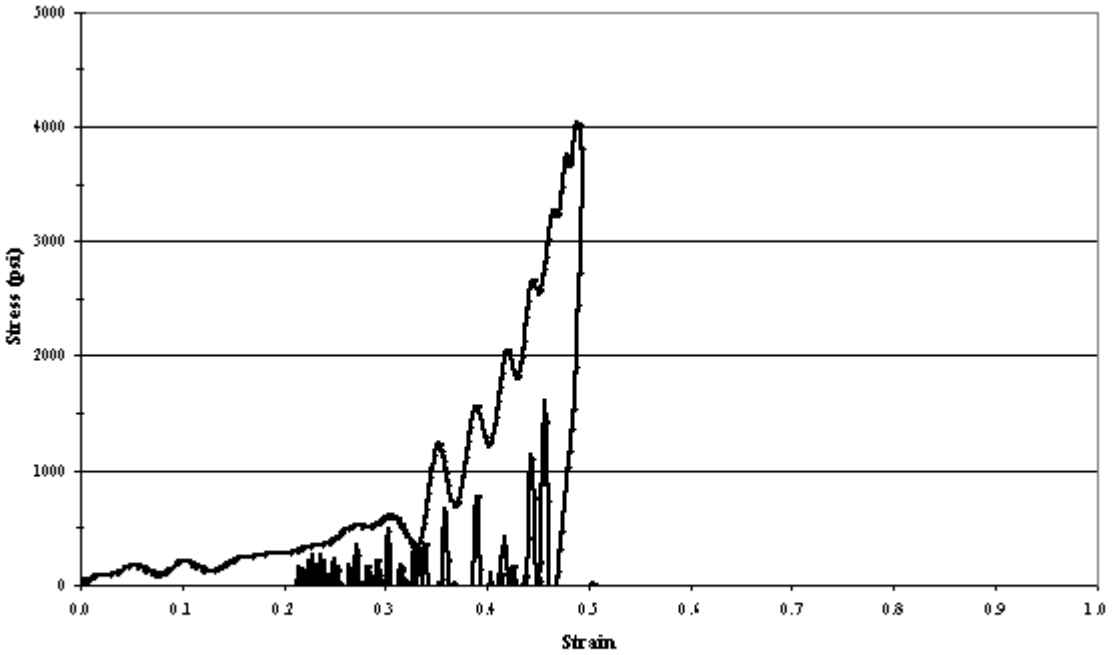

Figure 36. Second Series Impact Test Results for Hot Moist Specimen CT29 with Load Perpendicular to Plane of Celotex Sheets.

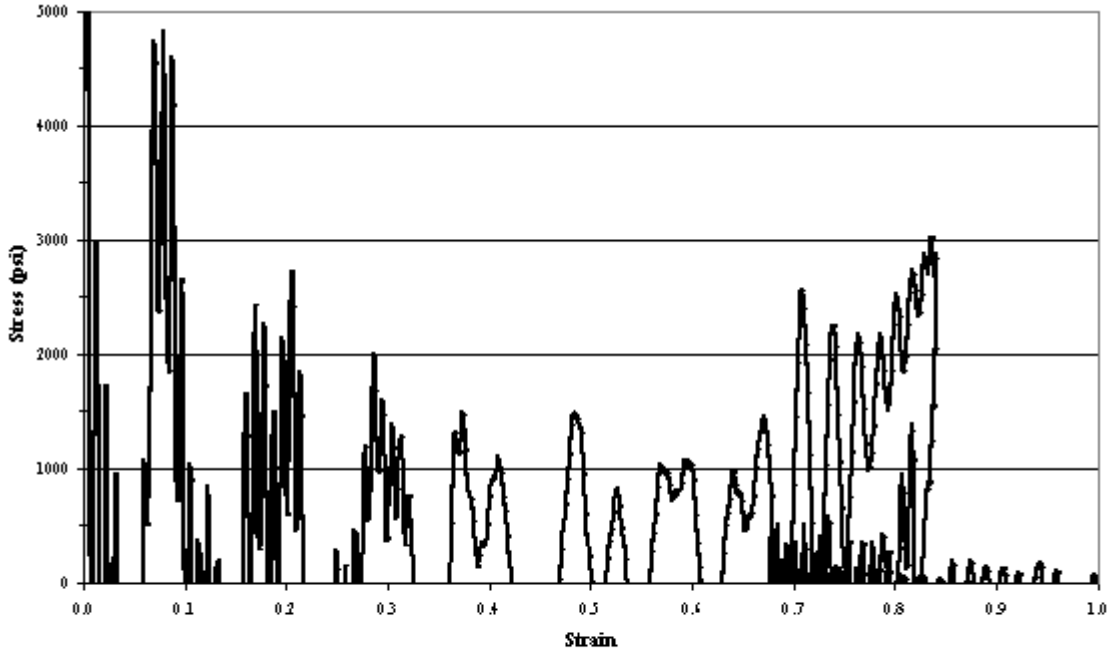

Figure 37. Second Series Impact Test Results for Hot Desiccated Specimen CT20 with Load Parallel to Plane of Celotex Sheets.

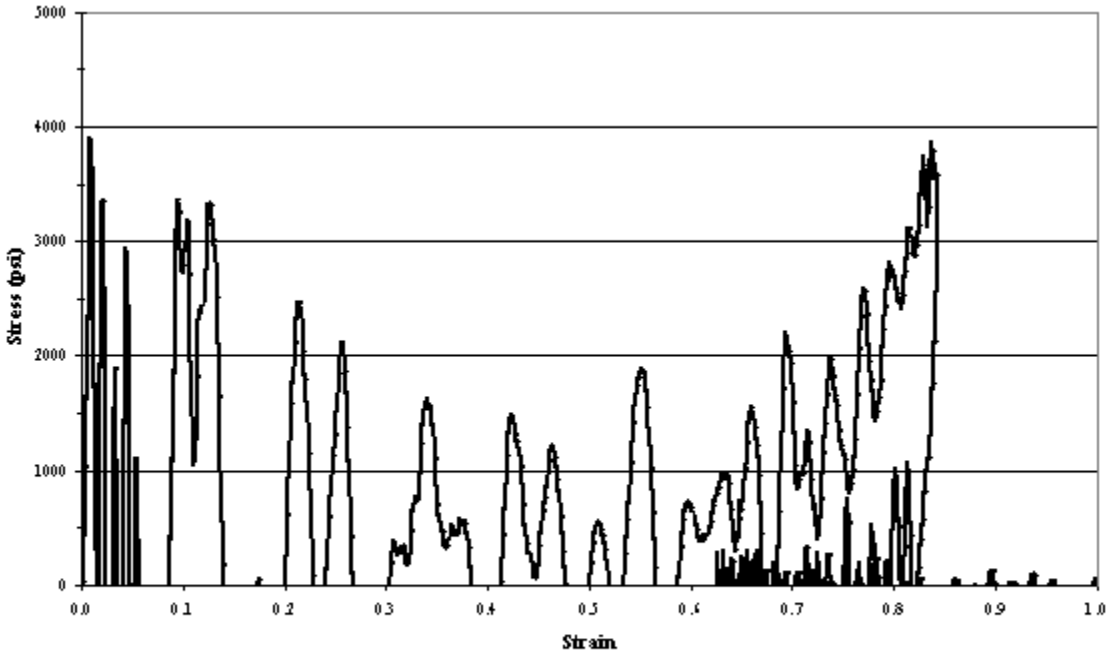

Figure 38. Second Series Impact Test Results for Hot Desiccated Specimen CT33 with Load Parallel to Plane of Celotex Sheets.

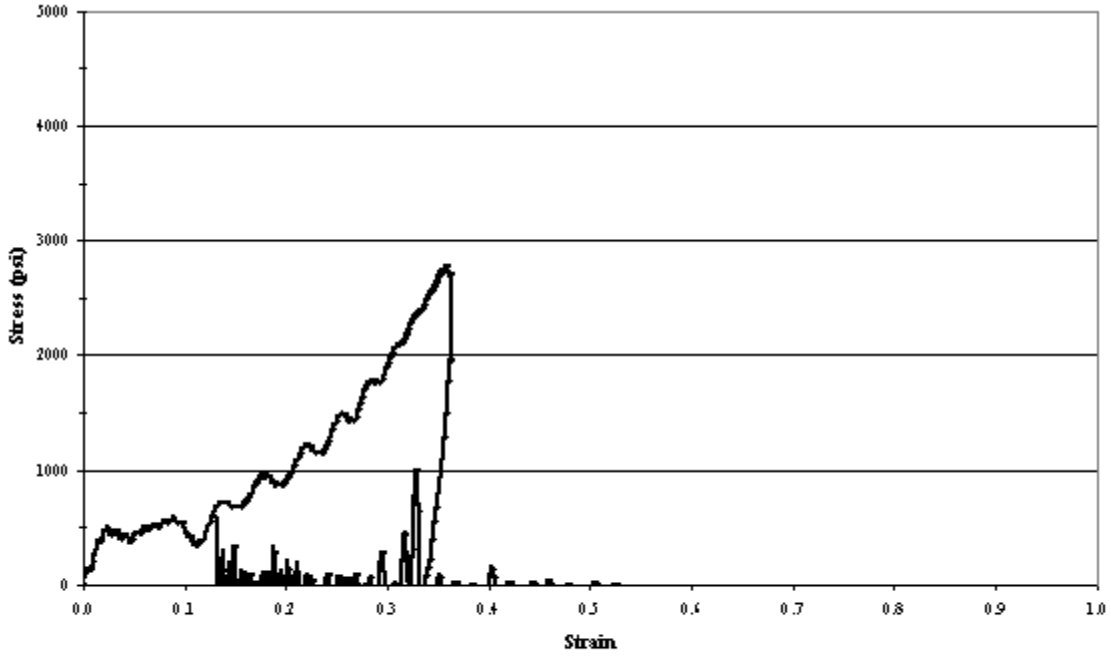

Figure 39. Second Series Impact Test Results for Hot Desiccated Specimen CT34 with Load Perpendicular to Plane of Celotex Sheets.

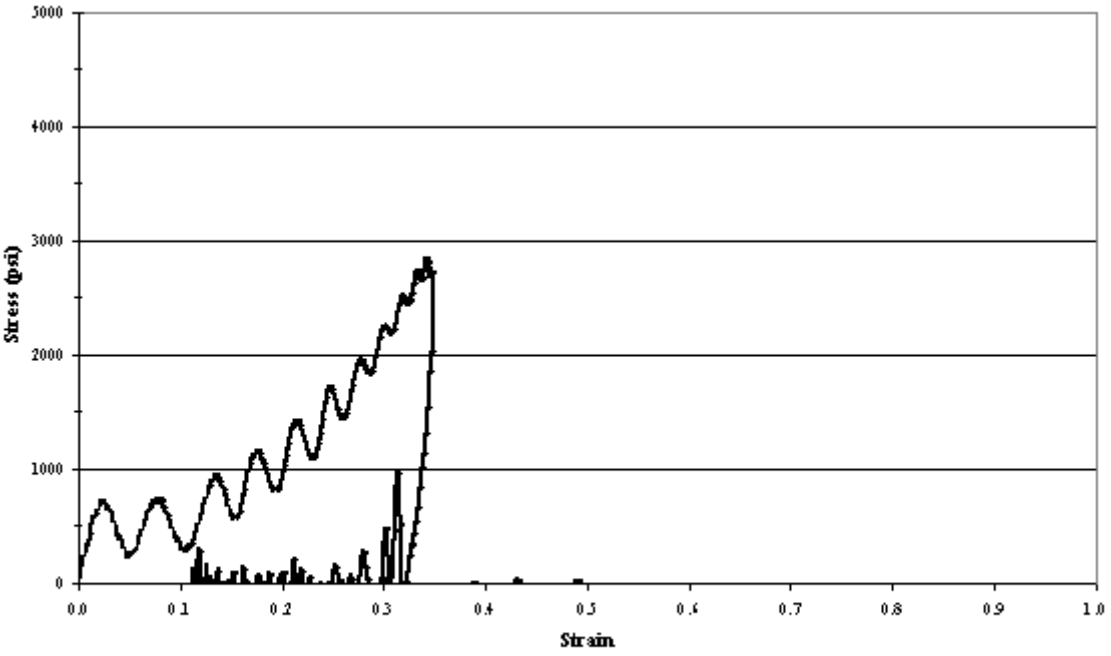

Figure 40. Second Series Impact Test Results for Hot Desiccated Specimen CT36 with Load Perpendicular to Plane of Celotex Sheets.

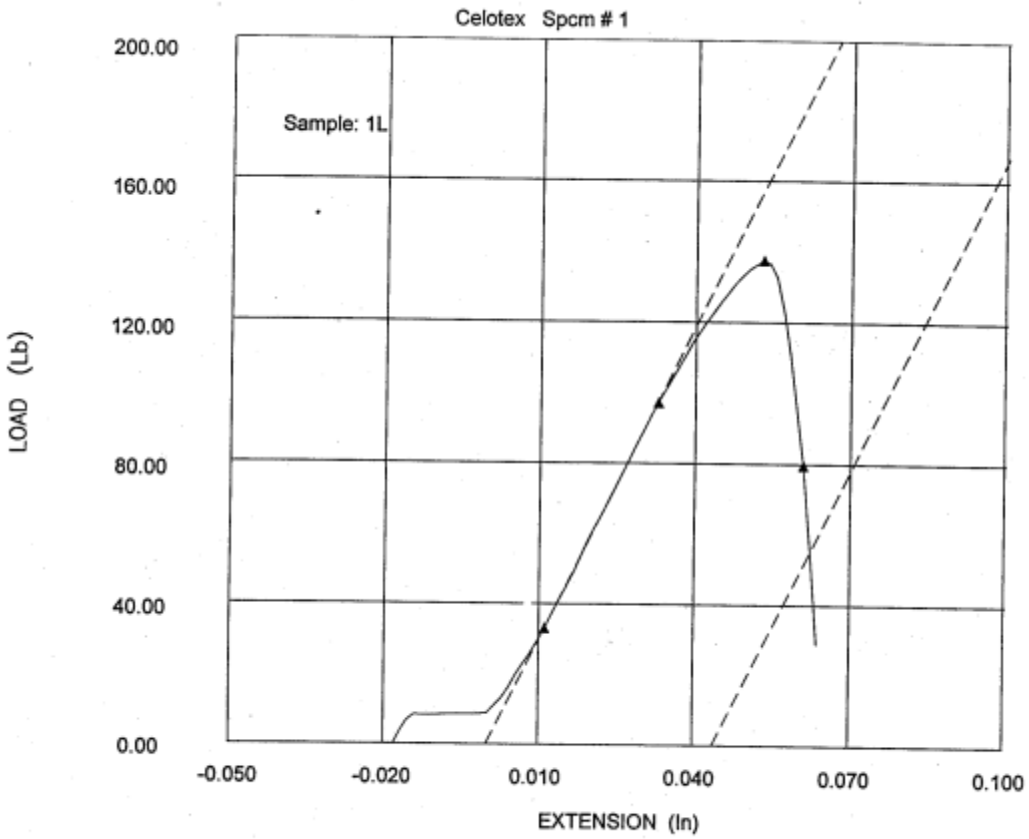

Figure 41. Typical results for single layer, in plane tensile test for Celotex.

CT33 - Dry Heated Vertical

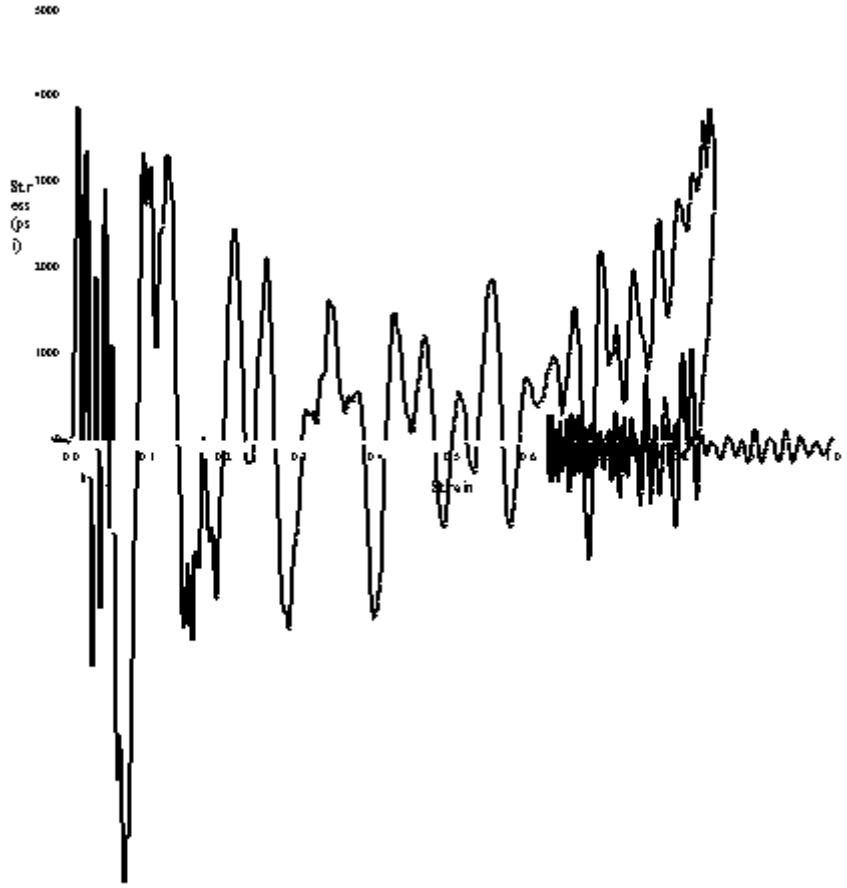

Figure 42. Full oscillation for CT33